Improving archaeomagnetic dating through new data acquisition and method development

Allington, Megan

2023

Document Version:
Publisher's PDF, also known as Version of record

Link to publication

Citation for published version (APA):
Allington, M. (2023). *Improving archaeomagnetic dating through new data acquisition and method development*. [Doctoral Thesis (compilation), Quaternary Sciences]. Lund University (Media-Tryck).

Total number of authors:
1

LUNDQUA THESIS 96

Improving archaeomagnetic dating through new data acquisition and method development

MEGAN L. ALLINGTON
QUATERNARY SCIENCES | DEPARTMENT OF GEOLOGY | LUND UNIVERSITY 2023

LUNDQUA THESIS 96

Improving archaeomagnetic dating through new data acquisition and method development

Megan L. Allington

LUND UNIVERSITY

Quaternary Sciences
Department of Geology

DOCTORAL DISSERTATION
by due permission of the Faculty of Science, Lund University, Sweden.
To be defended in Pangea, Geocentrum II, Sölvegatan 12
on Friday 26th May 2023 at 09.15.

Faculty opponent
Dr. Anita Di Chiara
INGV, Italy

Cover Photograph: Megan L. Allington (Buhera District, Zimbabwe)

Paper I Photograph: Reproduced with permission from the Ness of Brodgar Trust

Paper II Photograph: Megan L. Allington (Khami Ruins, Zimbabwe)

Paper III Photograph: Reproduced with permission from Brian W. Hayward © 2009

Quaternary Sciences
Department of Geology
Faculty of Science

ISBN 978-91-87847-78-3 (print)

ISBN 978-91-87847-79-0 (pdf)

ISSN 0281-3033

Printed in Sweden by Media-Tryck, Lund University, Lund 2023

Organization

LUND UNIVERSITY
Department of Geology
Sölvegatan 12
SE-223 62 Lund
Sweden

Author(s): Megan L. Allington

Document name

DOCTORAL DISSERTATION

Date of issue: 2023-04-28

Sponsoring organization

Title and subtitle: Improving archaeomagnetic dating through new data acquisition and method development

Abstract:

The Earth's magnetic field (or geomagnetic field) has been measured for hundreds of years, starting with maritime observations from logbooks for navigation purposes to present day real-time recording by satellites. From these records, the geomagnetic field variation throughout recent time is well-understood. In order to study longer term field variations (on the scale of hundreds to thousands of years), it is necessary to use indirect methods of observation of the geomagnetic field, recovered from lavas and burnt archaeological clays. Reconstructions of the geomagnetic field based on such archaeo-/ palaeomagnetic data can be used both to date certain archaeological and geological materials and to study deep Earth processes where the field is generated. However, the currently available archaeo-/ palaeomagnetic data are not geographically nor chronologically well-distributed. The first aim of this thesis is therefore to provide new archaeomagnetic field determinations from locations that are currently under-represented (either spatially or temporally) in the geomagnetic field records, including southern Africa, New Zealand and the Orkney Isles, UK. New geomagnetic field intensities have been collected from each targeted location and in addition, new geomagnetic field directions from New Zealand have also been produced. Archaeomagnetic dating is challenging in data sparse areas such as these, due to large and often unknown uncertainties of either the data (due to non-ideal formation/ preservation conditions) or the geomagnetic reference curves or both. The second aim of this thesis is to address such problems by introducing alternative methodologies for archaeomagnetic dating, (i) accounting for unknown uncertainties and (ii) using alternative constraints, such as the rate of change of the geomagnetic field to be able to provide chronological information.

Key words: geomagnetic field, archaeomagnetism, palaeomagnetism archaeomagnetic dating

Classification system and/or index terms (if any)

Supplementary bibliographical information | Language: English

ISSN and key title: 0281-3033 LUNDQUA THESIS | ISBN: 978-91-87847-78-3

Recipient's notes | Number of pages: 110 | Price

Security classification

Signature: MAllington Date: 2023-04-04

Contents

List of Papers

This thesis is based on the following publications and manuscripts:

Paper I
Obtaining archaeointensity data from British Neolithic pottery: A feasibility study.
Allington, M. L., Batt, C. M., Hill, M. J., Nilsson, A., Biggin, A. J. and Card, N. (2021)
Journal of Archaeological Science: Reports, 37, 102895, https://doi.org/10.1016/j.jasrep.2021.102895

Paper II
New Archaeointensity Results from the Iron Age in Southern Africa.
Allington, M. L., Lindahl, A., Hill, M. J., Suttie, N. and Nilsson, A.
Manuscript.

Paper III
Constraining the Eruption History of Rangitoto Volcano, New Zealand, using Palaeomagnetic Data.
Allington, M. L., Nilsson, A., Hill, M. J., Suttie, N., Daniil, D., Hjorth, I., Aulin, L., Augustinus, P. C. and Shane, P.
Submitted to *Quaternary Geochronology.* In review.

Acknowledgements

This PhD has been a long and sometimes difficult journey, even ignoring the global 'shut down' half-way through it all, but I am grateful for everyone who I've met along the way.

First of all, I would like to thank Andreas. I know it has been a slow journey at times but thank you for always offering help and support.

Mimi, thank you for all the support. I will always appreciate all the help you have offered with my work and your kind comments when things look a bit down. In extension, thank you to everyone at the Liverpool Geomagnetic Lab for being so welcoming during my visits.

Thank you Anders, especially for the accompanying me during the Africa trips and for using your house as a base. Not sure I am as thankful to the roosters for the 5 am wake-up calls though…

I would also like to thank every co-author and collaborator, thank you for being interested in my projects, and all the helpful insight and feedback.

To all the PhD students, both past and present, thank you for creating such a fun environment here at the department. An extra thank you is deserved for Anton (very welcome), Miriam, Josefin and Inda for being such good company throughout my time here.

I would also like to thank everyone who I've ever shared an office with here, but Sofia and Lena deserve a special mention, thank you for all the fun, support and gossip (haha) you both offered over the years.

To everyone at Geocentrum II, especially those who have ever helped me answer anything credit, admin or technology related. The department wouldn't be the same without you!

To the Pokémon TCG community, both in Malmö and Copenhagen, thank you for providing a very welcome distraction, especially in the final stretch.

To Mum and Holly, and all my other friends and family back in England, thank you for always providing laughs (and love).

Till familjen Härling, tack för att ni har välkomnat mig in till er familj här i Sverige då jag inte alltid haft möjligheten att träffa min egen familj.

Jesper, I don't know where I would be without you during all of this. I could never thank you enough.

Abbreviations

AF: Alternating Field

ARM: Anhysteretic Remanent Magnetisation

CRM: Chemical Remanent Magnetisation

IRM: Isothermal Remanent Magnetisation

MD: Multi-Domain (grain)

MMTD: Magnetic Measurements Thermal Demagnetiser

MWS: Microwave System

PSD: Psuedo-Single Domain

pTRM: Partial Thermoremanent Magnetisation

SAA: South Atlantic Anomaly

SD: Single Domain

SV: Secular Variation

SVC: Secular Variation Curve

T_b: Blocking Temperature

T_c: Curie Temperature

TRM: Thermoremanent Magnetisation

VRM: Viscous Remanent Magnetisation

1. Introduction

The Earth's magnetic field (the geomagnetic field) is vital to multiple systems on Earth. Perhaps the most important function of the geomagnetic field is providing a shield against harmful cosmogenic radiation, both from the Sun and from outside the galaxy. By deflecting cosmogenic radiation, the field also protects satellites from excessive exposure to charged particles ejected from the Sun, which can cause interference with the electronic equipment on-board (e.g.- Dang et al., 2022; Heirtzler, 2002). Living organisms, such as birds, butterflies and even bees, also use the geomagnetic field for navigational purposes (Lohmann et al., 2022).

The geomagnetic field was first measured in China as early as 720 AD (Smith & Needham, 1967), with measurements from maritime navigation becoming common from the 16th Century (Jackson et al., 2000). Today, we have real-time direct measurements from satellites, which provide information about geomagnetic field strength and direction (e.g.- Friis-Christensen et al., 2006; Primdahl et al., 2006). However, to reconstruct variations in the geomagnetic field direction and/or strength before these direct observations began and to understand the development of the Earth's magnetic field over longer timescales, indirect recordings of the geomagnetic field are required. Magnetic minerals within sediments, clays and lavas can record snapshots of the magnetic field. These materials, when analysed can give information about the past geomagnetic field and its behaviour through time (e.g.- Downey & Tarling, 1984; Hoye, 1981). These data are compiled into regional reference curves (e.g.- Hervé et al., 2013a, 2013b; Kapper et al., 2020; Zananiri et al., 2007) or regional/global geomagnetic field models (e.g.- Constable et al., 2016; Di Chiara & Pavón-Carrasco, 2022; Hellio & Gillet, 2018; Nilsson et al., 2022; Schanner et al., 2022). To understand the full scale of the behaviour of the geomagnetic field at the source region (the liquid outer core) requires data from all around the world, and throughout geological time.

Geomagnetic field reconstructions can be used to date objects of an unknown age by providing a geomagnetic field reference (to which measurements from the object can be compared) in regions and time periods where the models are sufficiently well-constrained by independently dated records (Pavón-Carrasco et al., 2011). This is called palaeomagnetic dating. When considering archaeological timescales (hundreds to thousands of years), the term archaeomagnetic dating is often used instead.

Geomagnetic field reconstructions also have several applications in Earth Science, some examples include studying processes in Earth's deep interior where the field is generated (e.g.- Mound & Davies, 2023; Nilsson et al., 2020), and to reconstruct solar activity over millennial timescales based on cosmogenic radionuclide data (e.g.- Muscheler et al., 2016; Nguyen et al., 2022).

Figure 1A. shows the distribution of archaeomagnetic direction and intensity measurements dated between 5000 BC and 2000 AD. The dichotomy between the two hemispheres is clear, with the Northern Hemisphere containing the most data, especially in the European region. We see that the Southern Hemisphere is underrepresented in the available dataset at present. Figures 1B. and 1C. show how the archaeomagnetic data are distributed over the past 7000 years. It is clear that the data are distributed unevenly throughout time, with the majority of the data being from the past 2000 years.

The aim of this thesis is to generate new archaeomagnetic data from archaeological artefacts and volcanic rocks from where data coverage is currently sparse, including regions where there is little to no pre-existing data, and specific time periods where there is currently a deficit. This new information will allow geomagnetic field models to become better constrained in the regions under investigation.

The second aim of this thesis is to develop alternative methods of archaeomagnetic dating from regions where the reference model and/or data uncertainties are poorly constrained. This includes (i) parameterising and integrating over the unknown (true) uncertainties and/or (ii) relying on statistical information about the rate of change of the field rather than model predictions.

Finally, the analysed samples are evaluated in terms of ability to hold a remanent magnetisation, or if there are any material properties that may prevent them providing a reliable archaeomagnetic estimate and how such properties can be detected through pre-screening routines.

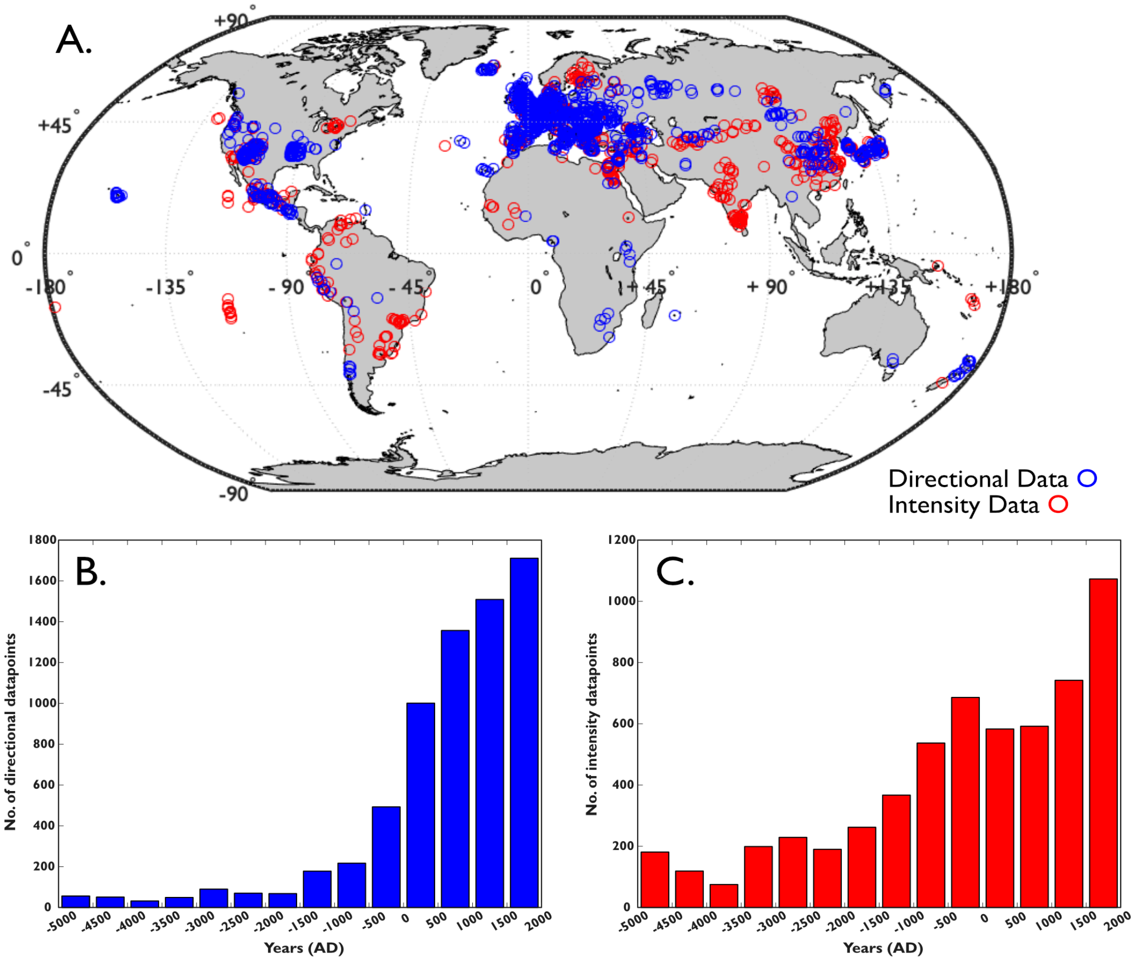

Figure 1: The locations of available archaeomagnetic data from archaeological artefacts and lavas globally over the past 7000 years. Data is taken from GEOMAGIA50v.4 (Brown et al., 2015) [accessed 2023-03]. Blue: Directional Data. Red: Intensity Data. B. Number of archaeomagnetic directions available over the past 7000 years. C. Number of archaeomagnetic intensities available over the past 7000 years.

2. Background

2.1. The Geomagnetic Field

The geomagnetic field is generated in the Earth's outer core, where kinetic energy from the motion of liquid iron is converted into magnetic energy. This conversion is self-exciting meaning that the geomagnetic field is perpetual due to this dynamo effect (a magnetohydrodynamic dynamo). This motion is attributed to thermal interaction between the core and mantle (Glatzmaier & Roberts, 1995).

The magnetic field at a point on the surface of Earth can be described with three values (Figure 2). Declination is defined as the angle between the geographic north and magnetic north, this value will be between 0° and 360°. Inclination provides the angle of dip, from horizontal, of the geomagnetic field and will be a value between -90° and 90°. Intensity gives the magnitude of the observed field. The field at the surface of Earth is predominantly dipolar (that is, consisting of two equal but opposite poles), with a small contribution by non-dipole components.

The geomagnetic field has the ability to reverse, where the north and south magnetic poles switch places. The geomagnetic poles are also known to wander towards the equator, potentially entering a reversed state (e.g.- González-López et al., 2021), and then returning to their original positions (Merrill & McFadden, 1994). Such events are known as excursions. Records of reversals have helped form a consistent chronological framework in geological archives (Lowrie & Alvarez, 1981), known as the geomagnetic polarity time scale (GPTS). The last

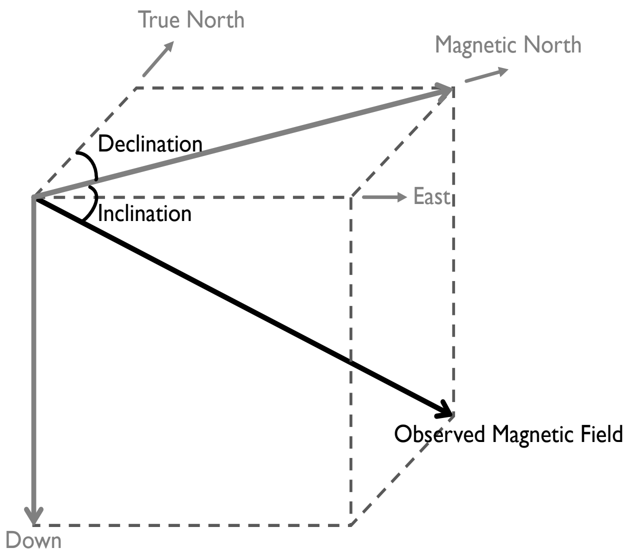

Figure 2: A vector plot showing how inclination, declination and intensity relate to both true and magnetic north.

reversal was the Matuyama/Brunhes reversal around 780,000 years ago (e.g.- Oda et al., 2000), as this thesis is focused on changes over the past few thousand years, reversalas are beyond the scope of this thesis.

Secular variation is the term used to describe variations in the strength (intensity) and direction (inclination and declination) of the geomagnetic field. For the past 160 years there has been a sharp decrease in the strength of the dipole field by 9% (Finlay et al., 2016), and an overall 25% decrease when looking at the past 2000 years (Nilsson et al., 2022).

Much of this recent decrease in dipole strength has been linked to the growth of an area of weak magnetic flux, known as the South Atlantic Anomaly (SAA), in the southern hemisphere over the Atlantic region (Figure 3). The SAA largely caused by the appearance of patches of opposite polarity flux at the Core Mantle Boundary (CMB) beneath the Atlantic (Olson & Amit, 2006). Dynamo simulations (Glatzmaier & Roberts, 1995) have shown that geomagnetic reversals are usually instigated by such flux patches of the opposite polarity appearing near the equator at the CMB and advancing towards to the poles. At present the observation record is too small to infer if the SAA is part of normal secular variation or a structure that is more abnormal (possibly linked to a geomagnetic field reversal or excursion), although there is evidence of similar geomagnetic field structures forming and disappearing over the past 9000 years, indicating that this may be reoccurring behaviour (Nilsson et al., 2022). The SAA is an area of interest, not only as a possible precursor to an imminent reversal, but due to the increased risk that a weak area of geomagnetic field can cause, such as the increase in charged solar particles. This is considered to be a potential risk to equipment and indeed people in spacecraft orbiting the planet (Heirtzler, 2002).

There are other characteristic geomagnetic field features observed in models over the historical era which may provide information on how the geomagnetic field is generated and maintained. This includes features such as intense equatorial flux patches below Africa which are consistently drifting westward (Finlay & Jackson, 2003). This westward drift is suggested to be due to movement in the core (e.g.- Aubert et al., 2013). Another feature are four intense flux patches ('flux lobes') seen at high latitudes, with two in each hemisphere, antipodal about the equator. They have remained relatively stationary over observable time suggesting that they may be coupled to temperature anomalies at the CMB (Gubbins et al., 2007). External forces such as mantle convection have a large effect as it brings cooler and geochemically distinct materials (such as oceanic plates) down towards the CMB. These cold slabs preferentially cool the core beneath subduction zones (Gubbins et al., 2015), which may influence the variation in field strength seen at the Earth's surface.

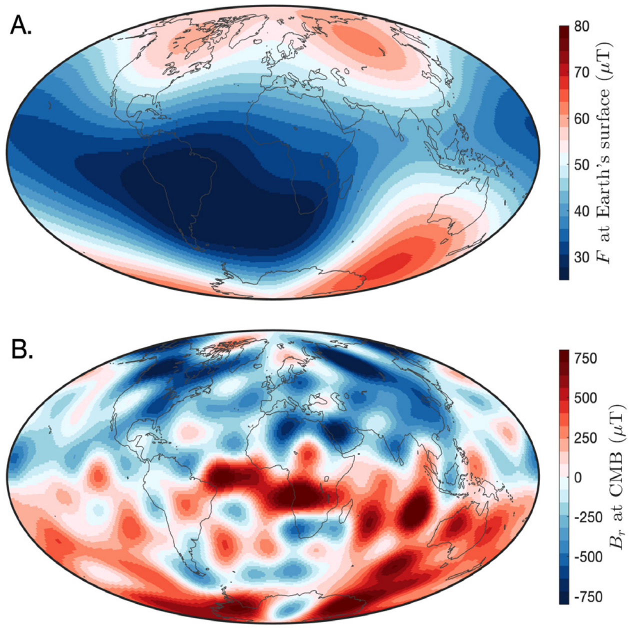

Figure 3: Maps showing A. The strength of the Earth's magnetic field at the surface of the Earth at 2020 AD. The South Atlantic Anomaly is the large patch of weak intensity (darker blue) in the Southern Atlantic. B. Shows the magnetic field at the core-mantle boundary showing four intense flux patches at high latitudes, two in each hemisphere, which are especially prominent in the Northern Hemisphere. The data shows the field behaviour from 2020 and is generated from the model COV-OBS.x2 (Huder et al., 2020).

2.2. Fundamentals of Magnetism

Types of Magnetism

The magnetic moment of an atom is fundamentally linked to the interactions between electrons spinning around their own axis and their orbit around a nucleus (as described in Dunlop & Özdemir, 1997). If an atom has full orbital shells of electrons, it will have no magnetic moment. In the presence of an external magnetic field, the object will have a weak induced magnetisation that is in the opposite direction of the applied magnetic field. This is called diamagnetism.

Atoms containing electron orbitals which are not all filled, and as such have free unpaired electrons present, have a magnetic moment. In a zero field, the individual atoms do not interact leading to a net zero magnetic moment for the material. However, if the material is in the presence of a magnetic field, a magnetisation is induced in the same direction as the applied field causing a positive net magnetic moment in the direction of the applied magnetic field. Objects exhibiting this behaviour are called paramagnetic materials (e.g.- Dearing, 1999).

Like paramagnetic materials, ferromagnetic materials also contained unpaired electrons, however in ferromagnetic materials the atoms are arranged in a crystalline lattice formation (Dunlop & Özdemir, 1997), which can lead to two adjacent atoms having electrons in the same orbit (Lanza & Meloni, 2006). The magnetic moments of these electrons align forming a magnetic domain (see Figure 4), which has a spontaneous magnetic moment, even when no magnetic field is present (Butler, 1992). If a ferromagnetic material is subjected to heating, thermal expansion of the material increases the interatomic distancing which decreases the strength of the magnetic moment between the electrons. If the applied temperature increases past a certain point, called a Curie temperature (T_c) (e.g.- Pasquale, 2019), the electron exchange forces drop to zero and the material loses this magnetisation and behaves paramagnetically. Ferromagnetic materials are considered to hold a permanent magnetisation as an input of energy is required for demagnetisation to occur, the temperature at which this point is reached is called the blocking temperature (T_b) (Tarling, 1983).

If the magnetic moment of domains in a material are of equal strength but occur in opposing directions, it results in zero net magnetisation (Figure 4). In this case a material is described as being antiferromagnetic. It is more common that the magnetic moments are not completely opposite, which is known as canted antiferromagnetism (e.g.- Dearing, 1999). Ferrimagnetic materials also have magnetic moments of opposing directions, however, the magnetic moments are significantly stronger in one direction (Figure 4), which leads to a small net magnetisation in one direction, which is capable of being held even in the absence of an external field (e.g.- Butler, 1992).

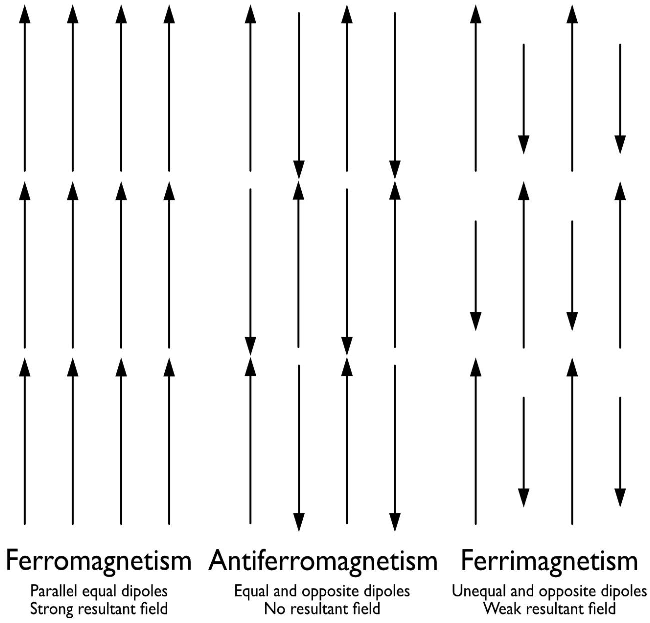

Figure 4: A schematic showing the magnetic dipole configuration when considering different types of magnetism.

Grain Size

Due to the crystalline structure of some grains, it is possible that the magnetic dipoles may have a preferred orientation, or easy axis (e.g.- Butler, 1992). Correspondingly, the direction of magnetisation will also follow this single, preferred direction. If the grain is small enough to contain only one magnetic domain, it is called single domain (SD). Such SD grains are capable of holding strong, stable magnetisations (Dunlop & West, 1969). If the crystalline structure gets large enough, the north and south poles of the dipoles begin to attract each other, causing the grain to break up into multiple, smaller domains (Tarling, 1983). Multi-domain (MD) grains record a weaker magnetisation as the magnetic moment of each domain are randomly aligned, causing a lower net magnetisation (Lanza & Meloni, 2006). Grains of an intermediate size can exhibit both SD and MD behaviours, known as pseudo-single domain (PSD). Generally, PSD grains have a small number of magnetic domains and record magnetisations and coercivity values of a similar magnitude to SD grains (Tauxe et al., 1996). Coercivity is a measure of how easily a magnetic remanence is removed (e.g.- Butler, 1992).

2.3. Acquiring a Magnetic Remanence

Archaeo- and palaeomagnetism are based upon the principle that certain objects that contain ferromagnetic grains can acquire a permanent magnetisation and retain this magnetisation over time (on the scale of millions of years). The initial magnetisation value that a sample has is known as the natural remanent magnetisation (NRM). This NRM depends on the magnetic fields and / or geological processes that the material has been exposed to (Koenigsberger, 1938). Commonly, this is the Earth's magnetic field, however local magnetic anomalies can also influence the magnetisation recorded in a sample (as described in Lanza & Meloni, 2006). The primary NRM is the initial remanent magnetisation a sample acquires often during the formation of the material. This remanent magnetisation can be imparted in a number of different ways, which are discussed below.

TRM and pTRM

A thermoremanent magnetisation (TRM) is acquired from cooling below the Curie temperature (T_c). This often occurs in situations where high temperatures are present, as such this is the most common acquisition method of a primary remanence for both clay-based archaeological artefacts and lavas (e.g.- Linford, 2006). An example is shown in Figure 5. As the material cools below the T_c, it switches from paramagnetic behaviour to ferromagnetic. The magnetic grains are now able to hold a spontaneous magnetisation, and if there is an ambient magnetic field present, the grains will gain a magnetisation aligned preferentially in the same direction (Lanza & Meloni, 2006). In general, the most dominant magnetic field, is the geomagnetic field, thus the direction and strength of the geomagnetic field at the time of the item cooling is recorded and preserved.

If a sample is re-heated to a temperature which is not high enough to remove the magnetisation from all grains, only a certain amount of grains will obtain a new magnetisation during cooling. This new magnetisation is a partial TRM (or pTRM) (e.g.- Tarling, 1983). This type of magnetisation is often seen in archaeological artefacts such as cooking ware, as the temperatures and duration of exposure to heat during cooking is often less than during the original firing of the pot. In this way, TRMs can be of particular interest to archaeologists as it can provide information on what the pot may has been used for (cooking or storage etc.) (e.g.- Francés-Negro et al., 2019; Karacic et al., 2016; Zhu et al., 2014).

DRM

Detrital Remanent Magnetisation (DRM) is the process of how sediments may record a magnetisation (Verosub, 1977). Magnetic grains (usually from surrounding bedrock eroding) that are in suspension in water, will align with the geomagnetic field as they sink to the bottom, and as the sediment is compacted, the grains lose the freedom to move, and retain the geomagnetic field information (Butler, 1992).

IRM

Isothermal Remanent Magnetisations (IRM) are magnetisations that are obtained by a short-term exposure to a strong field (as described in Butler, 1992). In nature, they are commonly caused by lightning strikes (e.g.- Dunlop & Özdemir, 1997). This can be identified in the laboratory, as they will record a much higher intensity and a random direction when compared to the rest of the outcrop under investigation.

CRM

A Chemical Remanent Magnetisation (CRM) is where a ferromagnetic phase is formed below the Curie temperature and acquires a remanence. This can be from the growth of a new ferromagnetic phase (e.g.- Baker & Muxworthy, 2023; Yamamoto, 2006) or the alteration of a pre-existing magnetic phase. A common cause of a CRM, in geological and archaeological materials is

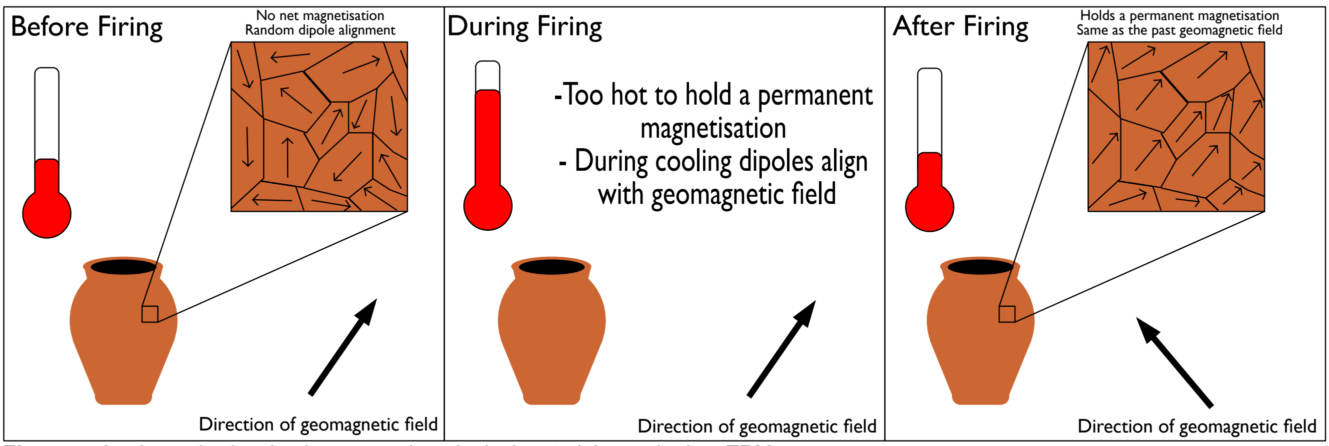

Figure 5: A schematic showing how an archaeological material can obtain a TRM

oxidation from weathering (e.g.- Nagata & Kobayashi, 1963; van Velzen & Zijderveld, 1995).

VRM

Viscous Remanent Magnetisation (VRM) is a secondary magnetisation (Lanza & Meloni, 2006) and it can be removed with low temperature demagnetisation. A VRM appears over time due to isothermal changes of the magnetised domains (Yu & Tauxe, 2006).

2.4. Magnetic Mineralogy

Determining the magnetic minerals contained within a sample can provide additional information on what the main magnetic remanence carriers are. The presence of certain magnetic minerals can also indicate if geochemical (or other types) of alteration has occurred since the sample obtained its magnetisation (e.g.- Barbetti et al., 1977; Krása & Herrero-Bervera, 2005). Therefore, the magnetic mineralogy can be indicative of how successful a palaeointensity experiment may be if attempted. It can also help identify if the NRM is primary or whether it has been replaced with a CRM etc., due to the identification of minerals often linked with weathering, such as goethite and maghemite (Table 1).

The most common magnetic minerals in terrestrial rocks are oxides and hydroxides of iron and titanium, with certain forms of titanomagnetites and titanohematites being some the most important in palaeomagnetism which are outlined in Table 1. The composition of titanomagnetites is defined by the quantity of titanium, TM0 (or magnetite) indicates no titanium and TM100 is ulvöspinel. A common form of titanomagnetite is TM60 (see Table 1), which is commonly found in rapidly cooled basaltic lavas (Dunlop & Özdemir, 1997).

Titanohematites, include minerals such as hematite and maghemite. Technically these minerals share the same composition, but the arrangement of the atoms is different (from Tarling, 1983). Maghemite is commonly formed from the weathering or oxidation of magnetite (Dunlop & Özdemir, 1997).

Table 1: A list of common magnetic minerals and associated Curie Temperatures. Values taken from Dunlop and Özdemir (1997).

Mineral	Chemical Formula	Curie Temperature (°C)
Magnetite	Fe_3O_4	580
Hematite	αFe_2O_3	675
Maghemite	γFe_2O_3	590 - 675
Titanomagnetite (TM60)	$Fe_{2\cdot4}Ti_{0\cdot6}O_4$	150
Goethite	FeOOH	120

2.5. Geomagnetic Field Reconstructions

Regional reference curves (secular variation curves) are comprised of a collection of geomagnetic field determinations from a specific region through time. These curves build a good foundation for archaeomagnetic dating (Lanos, 2004) (see Section 2.6). They are created with archaeomagnetic data that are independently dated (e.g.- radiocarbon dating). The datapoints are then relocated to a common latitude and longitude using the assumption of a dipole field, and a master curve is then constructed, typically using Bayesian methods (e.g.- Lanos, 2004).

As seen in Figure 1A. a large portion of archaeomagnetic data originates from the European region, and correspondingly there are many European countries with regional curves including Bulgaria (Kostadinova-Avramova & Jordanova, 2019; Kovacheva et al., 2014), France (e.g.- Hervé et al., 2013a, 2013b) and Italy (Tema & Lanos, 2021). Outside of Europe, regional curves are available from New Zealand (Turner et al., 2015a; Turner et al., 2020) and China (Cai et al., 2020). A benefit to regional curves is being able to select the highest quality data from a region to be input into the curve creation process, ensuring that archaeomagnetic dates that would come from these curves are more trustworthy.

Regional models are valid for larger areas than regional curves. They are constructed using the spherical cap harmonic analysis technique (e.g.- Pavón-Carrasco et al., 2009), which incorporate the data inside the region but also means data from larger distances can be added to help refine the model predictions. It also means that data does not need to be relocated, eliminating this source of error (Casas & Incoronato, 2007). Regional models are available in Europe (Pavón-Carrasco et al., 2021; Pavón-Carrasco et al., 2009) and Africa (Di Chiara & Pavón-Carrasco, 2022). There is also a regional model for the UK, ARCH-UK.1 (Batt et al., 2017), although that is constructed in the same process as a global model (see below) but with more weight applied for data from the UK.

Global geomagnetic field models combine large ensembles of data from all around the globe. Each model uses different criteria to accept and reject datasets but are far less restrictive than selection for a regional curve might be. Global models are created using data from archaeological materials, lava flows and sedimentary data (e.g.- Nilsson et al. 2022; Schanner et al., 2022). Some models only use the data from archaeological materials and lava flows, such as the ARCH*x*k models (e.g.- Korte et al., 2019) and COV-ARCH (Hellio & Gillet, 2018) as sedimentary data often causes a smoothing effect due to DRM acquisition being a gradual process (Roberts & Winklhofer, 2004).

Even when not including sediment data, global models often show lower amplitude due to inconsistencies in the data from different locations. However, in principle global models are able to incorporate information about large global scale field variations, in addition to the information gained from regional data used for regional models.

2.6. Archaeomagnetic Dating

Dating is very important in many research fields such as archaeology and geology. As the past geomagnetic field behaviour can be determined from archaeological artefacts, and there are models showing the variation of the geomagnetic field over time, it is possible to date an object by virtue of the geomagnetic field information it records. Theoretically, this method is possible for any fired clay or stone, such as hearths, bricks and pottery, however it requires detailed knowledge of the geomagnetic field behaviour for the appropriate time period.

In order to achieve a reliable age, the secular variation curve must be well-constrained, which requires that a large amount of measurements of independently dated materials to have been made in the region. As discussed in Section 2.5, there are a number of locations with well-constrained curves. It is also possible to use regional or global models, however, as they are smoother, the final date obtained may not be as precise as if a regional curve was used.

Archaeomagnetic dates can also be obtained using a Bayesian approach (Lanos, 2004). At a fixed time t, the archaeomagnetic measurement (in this case intensity) is assumed to be normally distributed $F_D \sim N(F(t), \sigma_D^2)$, where $F(t)$ is the unknown (true) geomagnetic field at time t and σ_D is the measurement uncertainty. The unknown geomagnetic field strength is in turn assumed to be normally distributed with mean $F_M(t)$ and variance σ_M^2, provided by a geomagnetic field reference curve, e.g.- a model prediction. The likelihood of the observation, F_D, at time t is then given by Equation 1 where the unknown variable F is eliminated through integration.

$$p(F_D|F_M,t) = \int_0^{+\infty} p(F_D|F,F_M,t) \cdot p(F|F_M,t) \cdot dF \tag{1}$$

3. Sites and Samples

3.1. The Ness of Brodgar

The Ness of Brodgar is a large archaeological site in the Orkney Isles, Scotland, United Kingdom (Figure 6). The site is part of the Heart of Neolithic Orkney World Heritage Site alongside other sites in Orkney that have large significance in UK archaeology. The site was initially discovered in 2010 from a ground-penetrating radar survey (Card, 2012). There have since been multiple field seasons excavating at the site. The Ness of Brodgar consists of nine different structures, enclosed by a surrounding wall. Finds such as painted walls and stone balls suggests that the Ness of Brodgar had some ritualistic significance alongside residential use (Card, 2018). The Ness of Brodgar is from the British Neolithic period (4000 BC-2000 BC), with radiocarbon dating analysis indicating that the site was used for 500 years, between 3000 BC and 2500 BC (Card et al., 2017).

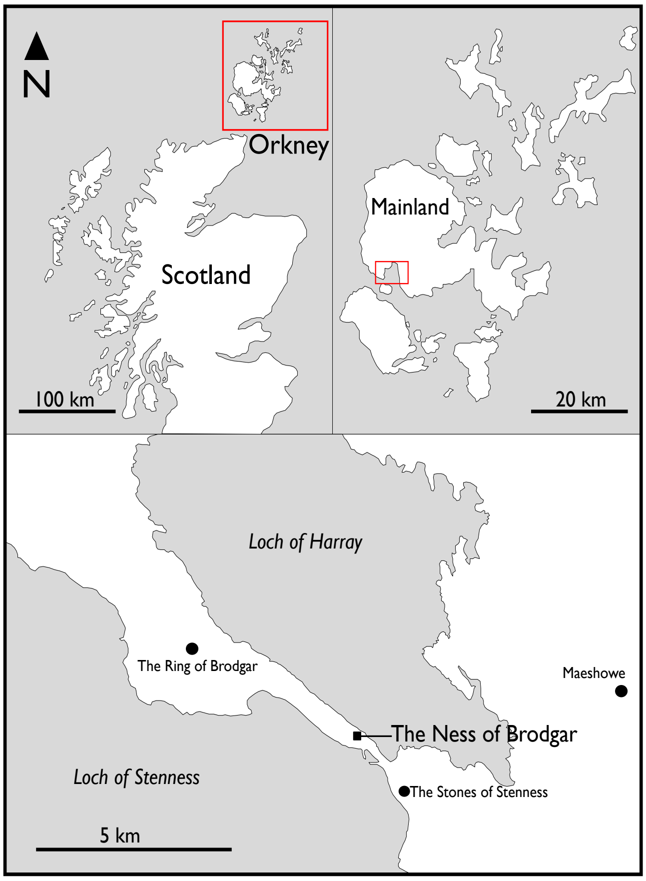

Figure 6: Map showing the location of the Ness of Brodgar

The sample set analysed here is composed of 25 pottery sherds from a few locations around the site, selected to look for potential variations that might be present (e.g.- for different tempers or preservation conditions). The Ness of Brodgar has significant chronological constraints already, including some of the pottery in this study having direct radiocarbon dates attached to them (Card et al., 2017).

3.2 Southern Africa

Southern Africa is a poorly covered region in terms of palaeomagnetic data, and due to the proximity of the region to interesting geomagnetic field features such as the SAA, it is an area that is of interest for more data collection. The pottery analysed here comes from the African Iron Age, defined as Early (200 – 900 AD), Middle (900 – 1300 AD) and Late (1300 – 1840 AD). There is material from South Africa, Botswana, Mozambique and Zimbabwe and the specific sites are marked in Figure 7. The majority of the sites included in this thesis are Zimbabwe Culture period sites (1220 AD – 1840 AD), which is commonly defined by the building of large, elaborate stone walls and a hierarchal class system. The sites studied range from large World Heritage sites to small habitations. Approximately 90% of the sample set consists of pottery sherds and the remaining 10% is burnt daga, which is a clay mixture used as a plaster to cover the walls and/ or floors of Iron Age houses.

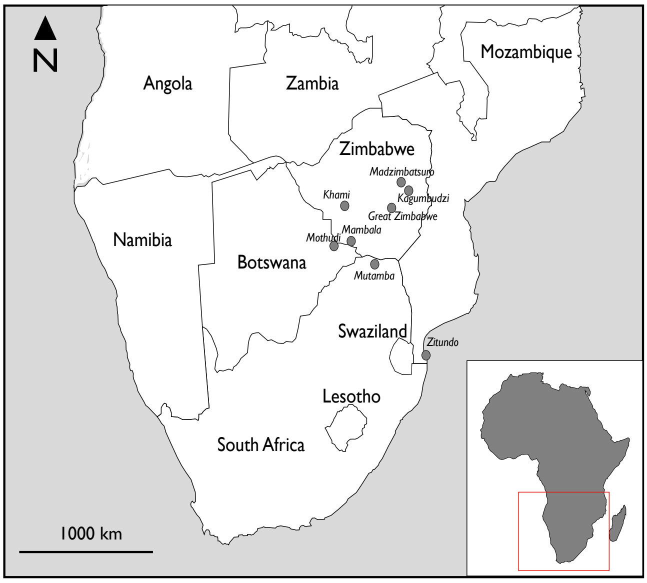

Figure 7: Map showing the location of the sites investigated in southern Africa.

3.3. Rangitoto Island Volcano

Rangitoto Island Volcano is a part of the Auckland Volcanic Field (AVF), which partly lies within the city of Auckland, New Zealand. The AVF has been active over the past 250,000 years and there are approximately 50 known eruption centres in the form of maars, scoria cones and tuff rings. Rangitoto Island Volcano (shortened to Rangitoto) is the youngest and largest in the field but the chronology of the eruption history of this volcano is still ambiguous. Given the proximity of Rangitoto to the city of Auckland (Figure 8), it is of crucial importance to understand the eruption history of Rangitoto to assess when and where the next eruption in the AVF may occur. The samples from Rangitoto are taken from a 140 meter long drill core taken from the western flank in 2014, originally described in Linnell et al. (2016). The top 128 m of the core is composed of at least 49 distinct massive basaltic lava flow units, which are interpreted to represent the main shield building phase.

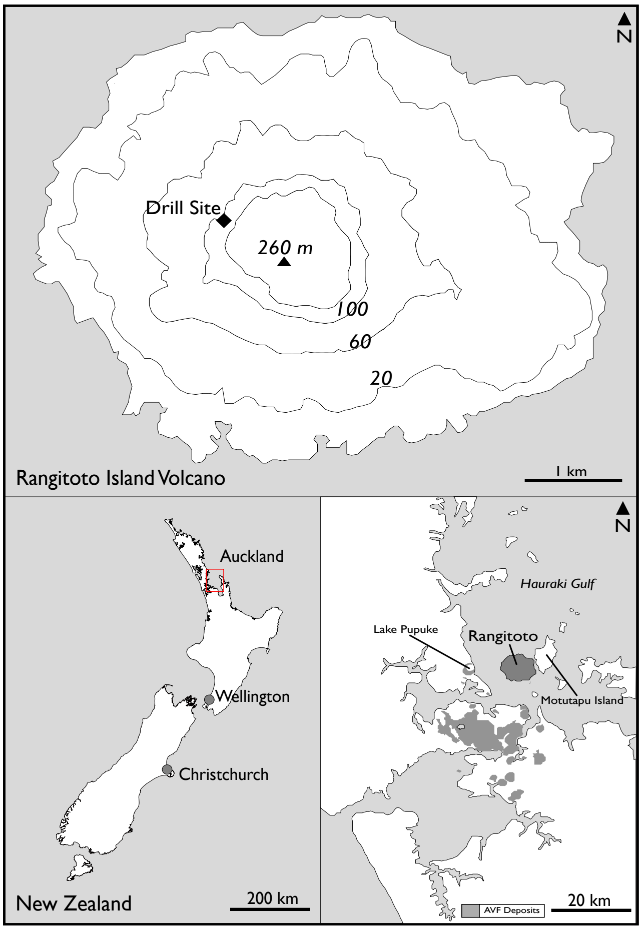

Figure 8: Map showing the location of Rangitoto and the location of the drill core site.

4. Methodology

4.1. Palaeodirectional Determinations

Demagnetising a sample requires an input of energy. There are a number of different types of energy that are commonly used in palaeomagnetism. The first is by thermal demagnetisation. A sample is heated in steps, with each progressive step removing the magnetisation of grains that have a blocking temperature below that temperature. The input energy can also be provided by an alternating magnetic field (AF) and microwaves.

Past geomagnetic field directions can only be obtained from in situ structures that have been excavated in a way that the orientations of the samples are recorded in some way. This limits the samples that can be analysed, when considering archaeological materials, pottery, for example, is unsuitable. Sampling must be done in a way to preserve orientation information, often done with sun or magnetic compasses (Tauxe et al., 2018).

In this thesis AF demagnetisation was utilised on the lavas from Rangitoto. However, the recovered intact core sections were not oriented with respect to geographic north, which means that only inclination data was recoverable. The retrieved drill core was subsampled for palaeomagnetic analysis by drilling perpendicular to obtain smaller cores, which were then further subsampled in slices with a water-cooled saw.

The Rangitoto samples were measured before and after AF demagnetisation in 5 mT steps up to 40 mT, then in 10 mT steps until a peak field of 80 mT was reached. The palaeodirections were calculated using principal component analysis (Kirschvink, 1980) using the NRM data between 15 to 80 mT.

4.2. Palaeointensity Determinations

Palaeointensity Experiments

Determining a past geomagnetic field intensity is similar in principle to obtaining a palaeodirection but for a palaeointensity determination, a new TRM (in a known field strength, H_{lab}) is acquired simultaneously, as the ancient TRM is removed in steps. This method was first developed by (Thellier & Thellier, 1959). The ratios of the original TRM ($TRM_{ancient}$) and the laboratory TRM (TRM_{lab}) are proportional to the ancient field strength ($H_{ancient}$), as shown in Equation 2.

$$H_{ancient} = \frac{TRM_{ancient}}{TRM_{lab}} H_{lab} \tag{2}$$

There are a number of different approaches to conducting an absolute palaeointensity experiment by heating the sample up in steps (e.g.- Tauxe et al., 2018). The first stepwise palaeointensity experiments were as early as Koenigsberger (1938), where the heating and cooling of the sample were both done in a laboratory field (in-field steps). Coe (1967) adapted the method to heat the sample in two successive steps, first in a zero-field environment (i.e.- demagnetising the sample) and then in a laboratory field (imparting a new TRM), so the order of steps becomes zero field-infield (ZI). It can also be done in reverse, so the first heating and cooling step is the one completed in a laboratory field (e.g.- Aitken et al., 1988) (i.e.- infield-zero field, or IZ).

In all versions of these experiments, it is possible to run repeat measurements of lower temperature steps to evaluate the sample. An ideal sample (that is not thermochemically altered) will have the potential to hold the same remanence throughout, so a pTRM check would record the same magnetisation as the original step (see Figure 9).

Often experiments use protocols that alternate the order of the steps. IZ followed by ZI (e.g.- Ben-Yosef et al., 2008; Tauxe & Staudigel, 2004), is referred to as the IZZI method. pTRM checks are often added after a pair of ZI steps, which is called the IZZI+ method (e.g.- Riisager & Riisager, 2001; Yu et al., 2004). These stepwise experiments are presented on an Arai plot (Nagata et al., 1963) (Figure 9), with the NRM ($TRM_{ancient}$) plotted against the TRM gained in the laboratory, with the line slope proportional to the ancient field (Equation 2). Figure 9 is an example of Arai plot of an ideal palaeointensity experiment. The IZZI method was intended to help identify (undesirable for palaeointensity analysis) MD grains by accentuating the behaviour they can cause in Arai plots, which makes a distinct 'zig-zag' effect (e.g.- Yu & Tauxe, 2005).

Heating up samples in steps multiple times can encourage sample alteration so other methods have tried to reduce the amount of times a sample is heated. These include the perpendicular field method (Kono & Ueno, 1977), which heats a sample only once after a low temperature step to isolate the NRM, in a field perpendicular to the direction of the NRM. The multi-specimen technique (e.g.- Dekkers & Böhnel, 2006; Hoffman & Biggin, 2005), use multiple samples from a homogenous unit (that has cooled simultaneously), and each sample is only exposed to a subset of the total number of heating steps. The Shaw method (Shaw, 1974), which uses AF to demagnetise an imparted TRM and an anhysteretic remanent magnetisation (ARM) so the sample is heated less repeatedly. An ARM is produced by a combination of a large AF field and a smaller DC field.

In this thesis, both thermal and microwave Thellier experiments were used to complete archaeointensity experiments. Both methods are known to provide comparable palaeointensity results (e.g. - Hill et al., 2002) and can both run protocols such as IZZI+. The microwave method is designed to help minimise alteration by targeting the magnetic grains causing the bulk sample to heat up less (Hill & Shaw, 1999), thus limiting the growth of secondary magnetic minerals (e.g.- Casas et al., 2005).

Certain behaviours that can bias a palaeointensity estimate should be addressed when evaluating archaeointensity results. The first is cooling rate. This occurs because materials may cool faster in the laboratory than the original heating (especially considering an environment such as pots in kilns etc.). This can lower the final archaeointensity estimate. Specific cooling rate experiments can be run so a correction can be applied to the final dataset (Fox & Aitken, 1980).The second is the anisotropy of the magnetic minerals which can influence an archaeointensity estimate. Separate experiments can be run to correct for this effect (Kovacheva et al., 2009; Rogers et al., 1979). Anisotropy is often induced during the formation of pottery as the clay is moulded.

There are a number of ways to evaluate the results from a palaeointensity experiment to determine the final accepted datasets based on statistical analysis of the experimental parameters and the Arai plots. Descriptions of commonly used parameters are shown in Table 2.

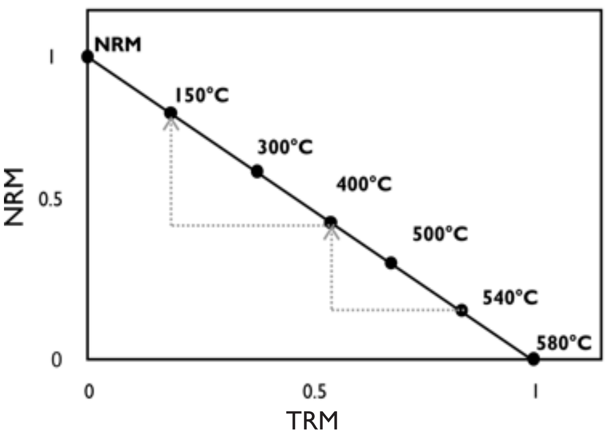

Figure 9: An ideal Arai plot with two pTRM checks.

Table 2: A description of common selection criteria used to evaluate archaeointensity experiments.l

Symbol	Criterion	Definition
N	Number	Number of points used from Arai plot to make the archaeointensity estimate.
f	Fraction	The fraction of the total NRM on which the archaeointensity estimate is based.
g	Gap	Gives a measure on the spacing between the points on the Arai plot.
β	Standard error	Error calculated from the slope of the Arai plot.
q	Quality	Assesses the overall quality of the result and is calculated by f*g/ β.
α	Alpha	Gives a measure on the scatter of the results.
γ	Gamma	Measures the angle between the applied field direction (H_{lab}) and the pTRMat the last step used for the best fit on the Arai plot. Often used as a indicator for how anisotropic a sample is.

There is currently no one consensus on what selection criteria to use for archaeo- and palaeointensity experiments. Popular criteria include SELCRIT2 (Biggin et al., 2007; Paterson et al., 2014), which is designed to be balanced yet comprehensive and help to remove undesirable MD effects, and CCRIT (Cromwell et al., 2015). CCRIT is designed to be stricter to ensure only high accuracy data is accepted by only accepting well-defined magnetisations.

Pseudo-Thellier Experiments

The psuedo-Thellier approach was originally developed by Tauxe et al. (1995) to determine relative palaeointensities from sedimentary rocks. The method requires the NRM of a sample to be demagnetised in steps. The sample is then remagnetised (in the same intervals) with an ARM. Although originally developed as a method to obtain relative palaeointensity estimates, it is possible to get absolute palaeointensity values from the method by multiplying by a calibration factor (de Groot et al., 2016). However, this method of determining palaeointensities is associated with additional uncertainties related to the calibration factor (e.g.- de Groot et al., 2013; Paterson et al., 2016).

Experiments Undertaken

The Ness of Brodgar samples were subject to both thermal and microwave analysis (although only the thermal Thellier analysis produced any accepted archaeointensity estimates). The microwave experiments were undertaken using a microwave system (MWS) consisting of a 14 GHz microwave system combined with a low temperature Tristan SQUID magnetometer. The thermal experiments were completed with an AGICO JR6 magnetometer and a Magnetic Measurements Thermal Demagnetiser (MMTD80). Both methods used the IZZI+ protocol (Yu et al., 2004) and a laboratory field strength of 50 µT. All results were evaluated using SELCRIT2 (Biggin et al., 2007; Paterson et al., 2014). All experiments on these samples were completed at the Geomagnetism Laboratory, University of Liverpool, UK.

The pottery sherds from southern Africa had thermal Thellier experiments completed on a 2G 760 magnetometer and an MMTD80 at the Palaeomagnetic Laboratory, Lund University using the IZZI+ protocol (Yu et al., 2004). The laboratory field was either 30 µT or 40 µT, dependent on the experiment batch a sample came from. The final selection criteria used here were the same as Tarduno et al. (2015), due to the similarities between the sample sets.

The Rangitoto lavas were analysed with the MWS consisting of a 14 GHz microwave system combined with a low temperature Tristan SQUID magnetometer at the University of Liverpool. Thermal Thellier experiments were done on a 2G 760 magnetometer and an MMTD80 at the Palaeomagnetic Laboratory, Lund University. All used the IZZI+ protocol and a laboratory field of 50 µT. All results were evaluated using SELCRIT2 (Biggin et al., 2007; Paterson et al., 2014). Psuedo-Thellier experiments were also completed on the lavas, using a 2G 760 magnetometer and a DC bias field of 50 µT. All samples were trimmed to fit the appropriate sample holders using a water cooled saw, in order to minimise the heat generated that the sample could become exposed to.

4.3. Magnetic Mineralogy Experiments

By exposing a sample to varying temperatures and magnetic field strengths, it is possible to determine which magnetic minerals are the NRM carriers, and if a sample is suitable for archaeomagnetic analysis. Below are a number of properties that were investigated in this thesis.

Curie Temperature

By heating, and subsequently cooling, a sample to high temperatures (in a set magnetic field), the Curie Temperatures (T_c) of the magnetic minerals present can be identified. A T_c can be identified as it produces an inflection point on the resulting thermomagnetic plot (e.g.- Tarling, 1983). If the heating and cooling path show the same behaviour, it implies that the sample has not undergone permanent magnetic mineralogy changes (i.e.- no alteration).

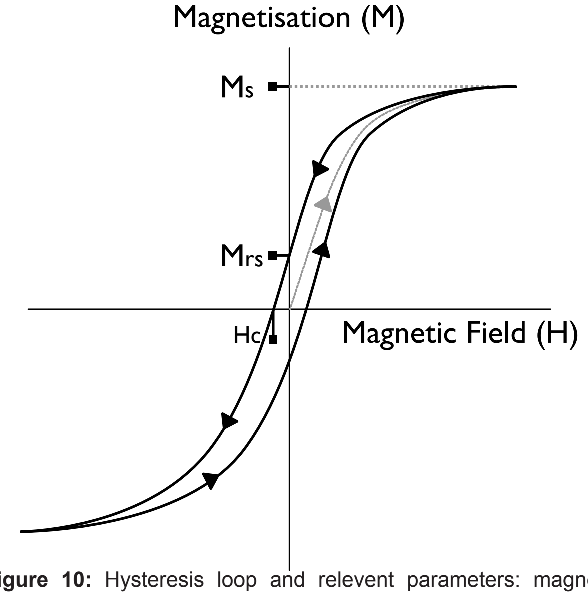

Figure 10: Hysteresis loop and relevent parameters: magnetic saturation (M_s), saturation remanence (M_{rs}) and coercivity (H_c). The grey dotted line shows the initial magnetisation curve. The black curves show the main hysteresis loop. The arrows show the direction of the applied field.

Hysteresis Properties

When exposed to a strong field, the magnetic saturation (M_s) is the point where the ferromagnetic grains in a material are completely magnetised in the applied field direction. A saturation remanence (M_{rs}) is the name given to the magnetisation that remains once the magnetic field is reduced to zero. The coercivity (H_c) is a measure of the width of the hysteresis loop and the coercivity of remanence measures how easily the magnetic remanence (M_{rs}) is removed when applying a field in the opposite direction to the initial applied field. These values are determined through hysteresis loop measurements (Figure 10), which shows the changes in magnetisation over varying magnetic fields, and an additional set of backfield measurements to determine the H_{cr}.

Magnetic Susceptibility

If a sample is heated up to above the Curie temperature and then cooled again, magnetic mineralogy can be inferred from the resulting curves. The susceptibility of ferromagnetic minerals sharply increase before the Tc, before decreasing drastically after the T_c is passed. This is called a Hopkinson peak (e.g.- Hrouda, 1994). If the heating and cooling curves do not follow the same path (i.e.- irreversible behaviour), it implies that the magnetic minerals have altered, such as the inversion of one magnetic phase into another.

Magnetic Grain Size

The magnetic grain size can also be determined from a hysteresis loop. The remanence ratio (Mrs/ Ms) and the coercivity ratio (Hcr/ Hc) plotted against each other in a Day Plot (Day et al., 1977), which has defined limits for where SD, PSD and MD grains will plot.

Experiments Undertaken

The Ness of Brodgar samples were analysed with a Variable Field Translation Balance (VFTB) at the Geomagnetic Laboratory, University of Liverpool, UK. Analyses including thermomagnetic curves and hysteresis loops were performed. Rangitoto samples were also analysed on the VFTB. The sample preparation for the VFTB involved crushing approximately 150 mg of sample into a fine powder, and then inserting this powder into a sample holder.

The southern African pottery measurements were carried out using an MFK1-FA Kappabridge with a CS4 attachment to get temperature dependent magnetic susceptibility between room temperature and 700 °C. Sample preparation for this involved grinding approximately 0.5 cm^2 of a sample to a fine powder. Hysteresis loops were measured on a small amount (0.10 cm^3) of sample using a Princeton Measurements Corporation alternating gradient magnetometer (AGM M2900-2).

5. Summary of Papers

This thesis consists of three papers, which are summarised here, and attached as appendices. The distribution of work for each paper is given in Table 3, which is located after Section 7.

Paper I

Obtaining archaeointensity data from British Neolithic pottery: A feasibility study. M.L. Allington, C.M. Batt, M.J. Hill, A. Nilsson, A.J. Biggin and N. Card (2021) Journal of Archaeological Science: Reports, 37, 102895.

This study analysed 25 sherds of Neolithic Grooved Ware pottery with an aim to evaluate the performance of the material as a suitable magnetic remanence carrier for palaeointensity determinations. With the recent construction of the ARCH-UK.1 secular variation curve (Batt et al. 2017), there is a basis for archaeomagnetic dating by intensity to become routine in the future for this region. However, data coverage is sparse especially when considering older archaeological time periods, so this study is the first in the Neolithic period (4000 BC – 2000 BC) in the UK.

Two methods for determining palaeointensity estimates were trialled, both conventional thermal Thellier and microwave experiments (MWS), with the thermal Thellier being the only method to produce any accepted archaeointensity estimates. Firstly, the sample material was very friable and was more difficult to sample for the MWS, and more importantly the pottery exhibited unusual behaviour during the application of microwaves to the sample, which was determined to be due to the sample not absorbing the same amount of microwave energy each cycle. The thermal Thellier experiments produced three new archaeointensity estimates, all between 35 μT and 40 μT. These values are consistent with both the limited data available within a 15° radius of the Ness of Brodgar and the values predicted by ARCH-UK.1.

A number of recommendations are given for future analysis of similar materials from the Ness of Brodgar, including running preliminary demagnetisation experiments to identify samples with an undesirable magnetic overprint and using only thermal Thellier for palaeointensity determinations. This study showed it is possible to obtain geomagnetic field information from the UK Neolithic from pottery and this could provide a basis for improving our knowledge of geomagnetic secular variation during the archaeological past in the UK.

Paper II

New Archaeointensity Results from the Iron Age in Southern Africa. M. L. Allington, A. Lindahl, M. J. Hill, N. Suttie and A. Nilsson (Manuscript).

In this study, nine new archaeointensity estimates are presented from archaeological material from the African Iron Age (200 AD – 1840 AD). The samples come from southern Africa and the new archaeointensity estimates (ranging between 18 μT and 40 μT) are consistent with the other intensity data in the region (Neukirch et al., 2012; Tarduno et al., 2015).

This study was conducted in such a way to analyse a small number of samples from many different archaeological sites, as in a region that is data sparse as southern Africa, all new data can be informative. In order to illustrate this point, an example of archaeomagnetic dating using a sample from an investigated site in Botswana is evaluated. To account for the poorly constrained data uncertainties, associated with sample level data, the dating methodology was adapted to assign the obtained experimental error as a minimum error and to treat the true uncertainty as an unknown parameter, which is marginalized. The site was occupied throughout the entire Iron Age (200 AD – 1840 AD), with excavations focused on structures that are typical of the Zimbabwe Culture Period (1220 AD – 1840 AD). The results from the dating in this case, suggest a maximum probability that the sample dates to the later part of the Iron Age (from ~ 1200 AD onwards). This is concurrent with the knowledge about the excavations on site.

This minimum uncertainty adaptation is also able to give more realistic results in situations when the intensity estimates fall outside of model predictions, which should be considered in the future when using archaeomagnetic dating.

Paper III

Constraining the Eruption History of Rangitoto Volcano, New Zealand, using Palaeomagnetic Data. M.L. Allington, A. Nilsson, M.J. Hill, N. Suttie, D. Daniil, I. Hjorth, L. Aulin, P.C. Augustinus and P. Shane. In review. Quaternary Geochronology.

In paper III, a total of 203 palaeomagnetic directions and 57 palaeointensity estimates from Rangitoto volcano in the Auckland Volcanic Field (AVF) are presented. Due to the proximity of the AVF to the centre of Auckland, understanding the eruption history of all the surrounding volcanoes is vital for hazard planning and preparations. The length of the shield building phase of Rangitoto is currently uncertain, with estimates ranging from under 100 years to over 500 years.

This new palaeomagnetic field data was then used to statistically determine the length of Rangitoto's shield building phase, based upon realistic geomagnetic field rates of change derived from satellite era models. Using already available radiocarbon dates (Linnell et al., 2016) as a priori information allowed us to evaluate the minimum duration of the shield building phase required to account for the variation in field values between each lava flow.

The inclination results show variations of up to 10° between lava flows, and synchronous changes are also observed in the intensity data. If these changes observed in the lava flows are due to geomagnetic field variations alone, this would imply that the shield building phase would have lasted over 1000 years. When the length of the shield building phase is limited by the radiocarbon ages, the model suggests eruption lengths of over 100 years, with a most likely duration of 150 and 450 years.

6. Discussion

6.1 Analysis of Non-Ideal Samples

In archaeomagnetism, it is common to encounter samples that may not perform as expected in the laboratory. Here, each site is discussed and reasons for samples failing are suggested. It is also indicated if these sites seem like key locations to target in the future when trying to collect more data for geomagnetic field models.

The Ness of Brodgar

The material analysed from the Ness of Brodgar (Paper I) was particularly problematic. When requesting samples, there were a number of criteria that were outlined to ensure diversity within the sample set, including, that the samples should come from a variety of the structures that make up the Ness of Brodgar. A variety of pottery textures was also requested to account for the variety that can be seen in Grooved Ware (e.g.- Cowie & MacSween, 1999), mainly due to uneven firing or different tempers, which is usually sand or other small grains for pottery from the Ness of Brodgar (Towers & Card, 2015). Whilst this selection strategy ensured that the full range of pottery that can be found at the site was investigated, it may also have limited the sample set that was suitable for archaeointensity experiments as the majority of the pottery was very friable and unconsolidated.

Whilst it was still possible to prepare the samples for thermal archaeointensity experiments using tubes sealed with quartz wool and a sodium silicate solution, (e.g.- Gómez-Paccard & Pavón-Carrasco, 2018), it was much more laborious and time-consuming. It would be recommended that any future work on Ness of Brodgar ceramics follow a similar procedure by default.

The preservation conditions at the Ness of Brodgar are not ideal, as it runs on a small strip of land, surrounded by water (Figure 11). Soils with a high water flux and areas of high rainfall are identified as poor environments for archaeological artefact preservation (Crow, 2008). These conditions make mineral alteration more likely, which in turn can alter the buried materials, causing changes to the physical and chemical changes that were not present initially.

Due to the nature of open fires, not all pottery will have

Figure 11: A site photograph of the Ness of Brodgar. It is surrounded by two lochs (Harray and Stenness). Photograph reproduced with permission from the Ness of Brodgar Trust.

reached the same temperature during the firing period. From experimental work, TRMs obtained are more stable in the centre of the heating area, as the temperatures get the hottest (e.g.- Carrancho & Villalaín, 2011), so it is possible that not all samples obtained a full TRM during firing, making them more likely to alter with future heating.

Demagnetisation screenings and magnetic mineralogy experiments to remove non-ideal samples before any archaeointensity analysis begins is recommended. This is not a new procedure as such, but supports other studies that have suggested similar strategies (e.g.- Kondopoulou et al., 2017). Overall, the sample quality at the Ness of Brodgar is relatively poor and although this can partly be accounted for by specific sample preparation and testing, the success rates of archaeointensity experiments are likely to still be low.

Whilst Europe has seen multiple new archaeointensity results from 2020 onward, including a large dataset from Central Europe (Germany, Austria and Switzerland) (Schnepp et al., 2020a; Schnepp et al., 2020b). However, all these field determinations only date as far back as 1500 BC. The archaeointensity results from Paper I were the first produced in the UK from the British Neolithic period (4000 BC – 2000 BC). Archaeointensity records from GEOMAGIA50v.4 (Brown et al., 2015) [accessed 2023-03] have shown that no additional archaeointensity data in the same 15° radius around the Ness of Brodgar (as shown in Paper I), over the same time period has been added since this study was published in 2021, which emphasises the importance of these results. Although we note, some other European countries such as Greece have worked on similarly aged samples (Aidona et al., 2023).

As Orkney has such a wealth of Neolithic aged sites, it would be ideal to overcome the challenges encountered in this study in order to take advantage of the potential of this archaeologically rich area to grow the density of geomagnetic field determinations in such a data sparse time period.

Southern Africa

Preliminary demagnetisations (e.g.- Kondopoulou et al., 2017), did help raise overall archaeointensity success rates. A common reason for rejection of a sample was due to the magnetic remanence being overprinted. This is not uncommon in pottery (Francés-Negro et al., 2019), due to pots being used to cook food.

The archaeointensity estimates from the pottery were scattered and showed unrealistic rates of change of the geomagnetic field when using SELCRIT2 (Biggin et al., 2007; Paterson et al., 2014), which was the same selection criteria as used in the Ness of Brodgar study. However, when a stricter selection criteria was chosen, that might be more appropriate as it has been used before on Iron Age materials from southern Africa (Neukirch et al., 2012; Tarduno et al., 2015), the scatter (mostly from a couple of anomalously low intensity estimates) is considerably reduced. The reason for the low intensity points are not entirely clear, but suggestions such as cooling rate are unlikely as these factors would likely further reduce some of the already anomalously low intensity estimates (Fox & Aitken, 1980).

There is still plenty that can be done with the southern African material that was studied in this thesis. A more thorough magnetic mineralogy investigation could help identify any regional differences in clay and may help identify the sites and samples that might behave better (instead of/or in combination with demagnetisation experiments).

Rangitoto Island Volcano

It is a possibility that some of the intensity variation captured by the Rangitoto lava flows is geochemical in origin. Overall, we observe higher intensities (for both conventional and pseudo-Thellier) in geochemical zone 3, than both the surrounding zones (1 and 4) as defined by Linnell et al. (2016), although the change does not happen directly at the boundary edge. Whilst the isolated remanent magnetisation is most likely a TRM, there is not enough evidence to rule out chemical alteration to the flows, that may account for some of the observed downcore palaeointensity variations. Systematic errors associated with palaeointensities from volcanic rocks have previously been noted, such as in the 1960 Hawaiian lava flow which has been shown to consistently produce incorrect estimates (e.g.- Hill & Shaw, 2000; Yamamoto, 2006; Yamamoto et al., 2003). In the case of the 1960 Hawaiian flow, a likely cause is that the rocks alter and grow a CRM during heating in the laboratory which causes the palaeointensity estimate to be too high. Although, with MWS analysis, the same lavas underestimated the intensities (Grappone et al., 2019; Hill & Shaw, 2000).

The Rangitoto dataset has the potential to be an important record for the southern hemisphere and be a big contribution to future geomagnetic field constructions, if in the future a consensus is reached on the eruption history based on independent dates that are not under scrutiny, like the current radiocarbon dates, due to evidence of potential sediment re-working (Shane et al., 2013).

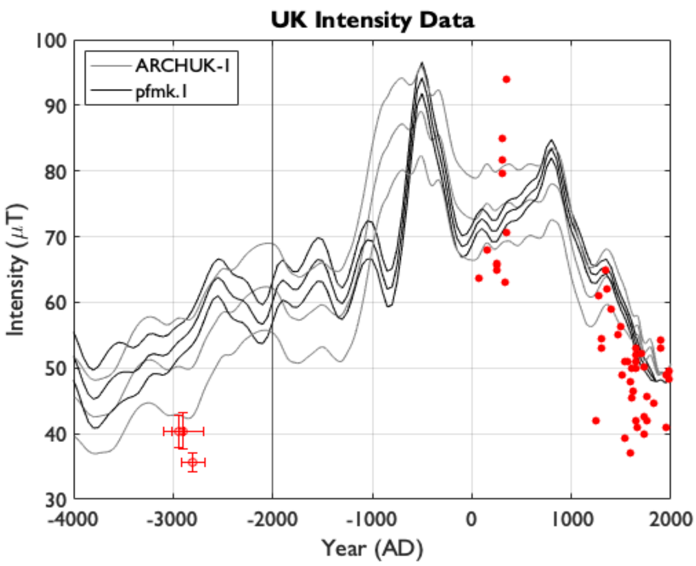

Figure 12: Plot showing the UK archaeointensity record (red points) that is included in the ARCH-UK.1 regional geomagnetic field model (Batt et al., 2017). ARCH-UK.1 is plotted with 1σ errors in grey, and the global model pfm9k.2 (Nilsson et al., 2022). The bold vertical line shows the limit of the British Neolithic period (-4000 to -2000 AD). The model is plotted for the location of the Ness of Brodgar. The data are from GEOMAGIA50v.4 (Brown et al., 2015) [accessed 2023-03]. The new Ness of Brodgar data is plotted for comparison.

6.2 Geomagnetic Field Models

There are three regional models/ regional curves that are especially relevant to this thesis. These will be discussed and compared with global models below.

ARCH-UK.1

This model is developed for UK data for the geographical range of latitudes 49°N to 61°N and longitudes 11°W to 2°E between 5000 BC to 2000 AD. For reference, the co-ordinates for Ness of Brodgar are 58.99°N, 3.21°W. The model, first introduced by Zananiri et al. (2007), is based on the ARCH*x*.k models (Constable et al., 2016), but global datapoints are down-weighted when compared to data from the UK. The UK archaeomagnetic record that ARCH-UK.1 based on, is comprised of a comprehensive set of archaeodirections, but there are no UK archaeointensity estimates before 0 BC (Figure 12). Consequently, there are very little UK data (only some directional data) controlling the model during the British Neolithic period (4000 BC – 2000 BC). However, the intensity data from the Ness of Brodgar still falls close the error bounds (2σ) of the model suggesting that the model is still providing reasonable information.

SCHAFRICA.DIF.4k

This regional model (Di Chiara & Pavón-Carrasco, 2022) contains Holocene aged data from 36 different studies on volcanic and archaeological materials from the continent of Africa (Di Chiara, 2020). A further 12 studies on sedimentary materials were not included, in part due to age inaccuracy and the smoothing of the sedimentary data. The model also contains data from outside of Africa (European data) to constrain part of the model limits.

NZPSVC1k

The New Zealand Palaeosecular Variation curve (or NZPSVC) is a set of records, both with a 1000 year model (NZPSVC1k) and a 10,000 year model (NZPSVC10k). The reference curves (Turner et al., 2015a; Turner et al., 2020) contains only data from New Zealand and are heavily influenced by the sediment records there (e.g.- Turner et al., 2015b).

Model and Curve Comparison

Figure 12 to 14 show how these reference curves / models compare to a variety of global models. From these figures it is clear that in data-sparse areas the model predictions are not consistent with each other. For example, SCHAFRICA.DIF.4k (Figure 13) is the only model that shows a dip in field strength around the year 1700. These

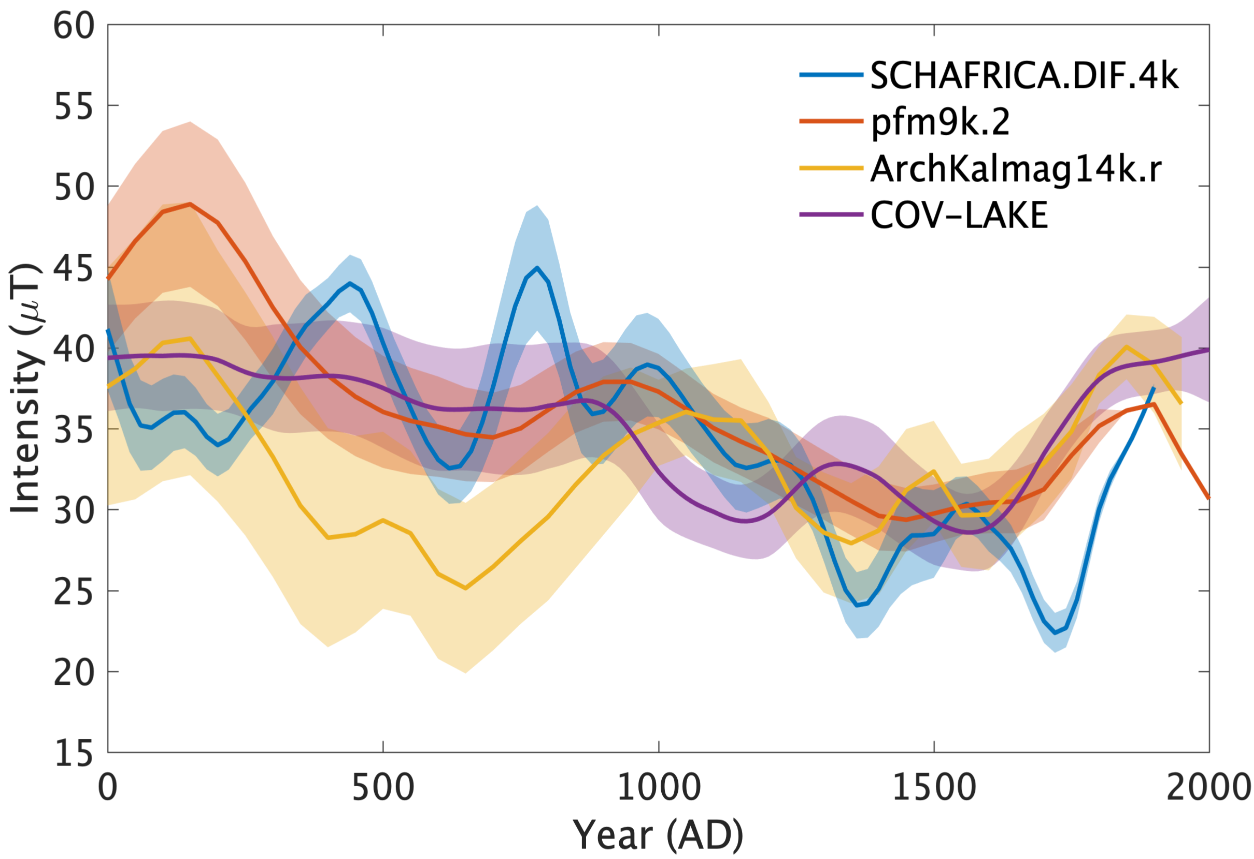

Figure 13: A geomagnetic intensity model comparison for 20°S, 30°E (which is close to central Zimbabwe). All models are plotted with 1σ error bounds. A. The regional model SCHAFRICA.DIF.4k (Di Chiara & Pavón-Carrasco, 2022) is plotted in blue . B. The global model pfm9k.2 (Nilsson et al., 2022) in orange. C. The global model ARCHKALMAG14k.r (Schanner et al., 2022) in yellow and D. The global model COV-LAKE (Hellio & Gillet, 2018) in purple.

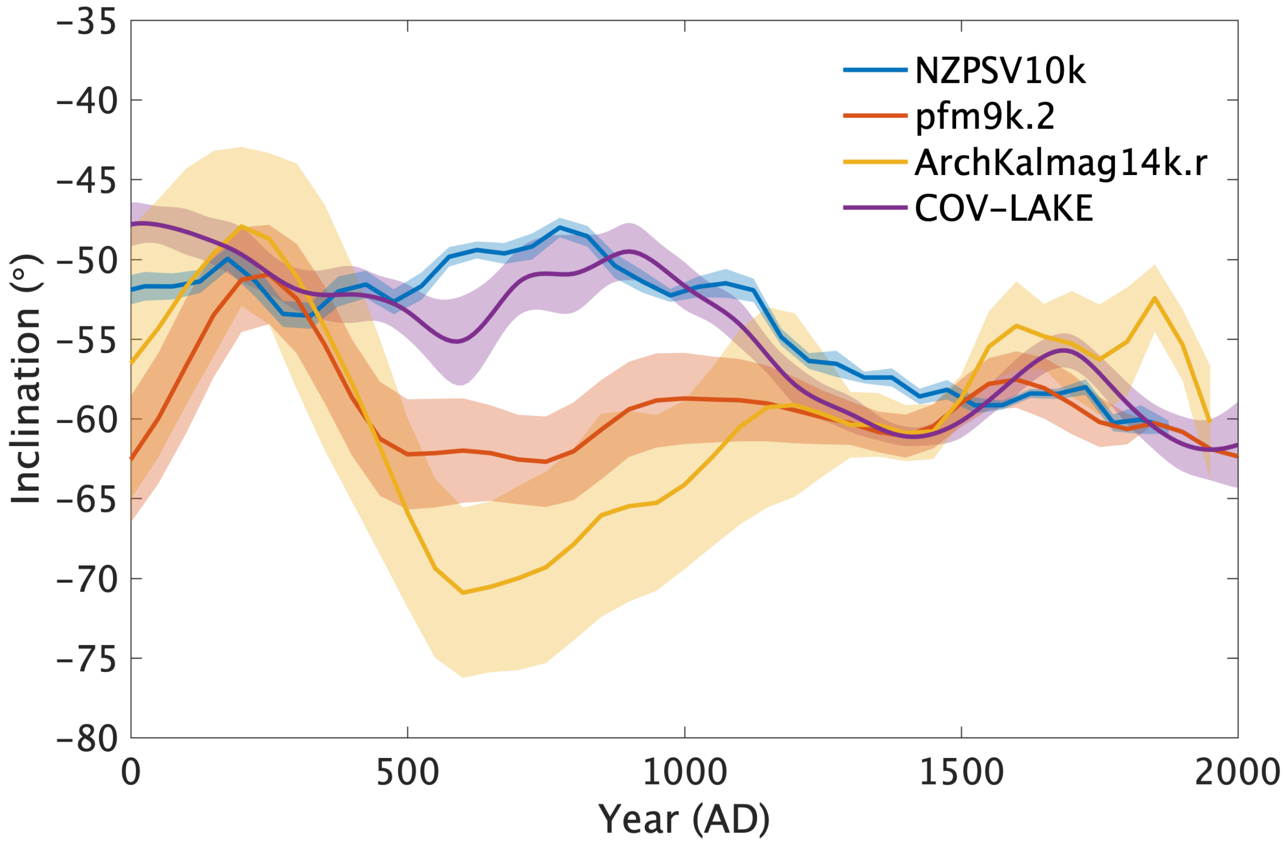

Figure 14: A geomagnetic model comparison for Rangitoto Island Volcano, New Zealand. All models are plotted with 1σ error bounds. A. The SV curve, NZPSV10k Turner et al., 2015; Turner et al., 2020, is plotted in blue . B. The global model pfm9k.2 (Nilsson et al., 2022) in orange. C. The global model ARCHKALMAG14k.r (Schanner et al., 2022) in yellow and D. The global model COV-LAKE (Hellio & Gillet, 2018) in purple.

differences are due to the selection of data for use in the model, how said data are weighted etc. It is currently not clear which model is more accurate, but overall it appears that the model uncertainties are underestimated in these areas.Therefore, comparing results from different models should be standard procedure.

6.3. Refining Archaeomagnetic Dating

Archaeomagnetic dating is viable in many locations, especially areas with specific SV curves. The locations in this thesis are purposefully from data-sparse regions (either geographically or chronologically), and as discussed in Section 6.2, model predictions in these areas can contradict each other suggesting that the model uncertainties are underestimated. Here, I suggest different approaches that can be utilised in order to still be able to provide age information for the analysed samples.

Accounting for Unknown Uncertainties

One important factor in archaeomagnetic dating is considering potential uncertainties and accounting for them in order to achieve a realistic final date. The Bayesian approach by Lanos (2004), and popularised by Pavón-Carrasco et al. (2011) with a MATLAB tool, is a very common approach to archaeomagnetic dating. In many situations this is appropriate, and a refined age can be achieved for the object under investigation.

In the scenario where model and / or data uncertainties are underestimated, it is possible that the method of Lanos (2004) will lead to over-precise age estimates. If a sample gives an archaeomagnetic intensity or direction that is not close to model predictions (e.g.- Figure 15), the method (Equation 1) will assign a narrow probability peak to the time period where the model and data are closest, even though they may not actually agree. This is because the method implicitly assumes that uncertainty estimates are correct.

One solution to this problem is to acknowledge that the uncertainties may not be correct and to integrate over the unknown (true) uncertainty from the data or model. A suggested modification is shown here (and in Paper II). Here, we assume that the true (but unknown) data uncertainty (ς) must be larger than or equal to the (minimum) experimental data uncertainty, σ_F. The minimum error value used here is the least-square error of the line fit from the Arai plot (Kosareva et al., 2020). Then following a suggestion by Sivia (2006), we assume a prior distribution for the true uncertainty of σ_F/ς^2 for $\varsigma \geq \sigma_F$ (Nilsson et al. 2018; Kosareva et al. 2020), and marginalise it to obtain Equation 3.

$$p(F_D|F(t),\sigma_D) = \frac{1}{\sigma_D\sqrt{2\pi}} \cdot \frac{1-e^{-\frac{\chi^2}{2}}}{\chi^2} \tag{3}$$

where:

$$\chi^2 = \frac{(F_D - F(t))^2}{\sigma_D{}^2}$$

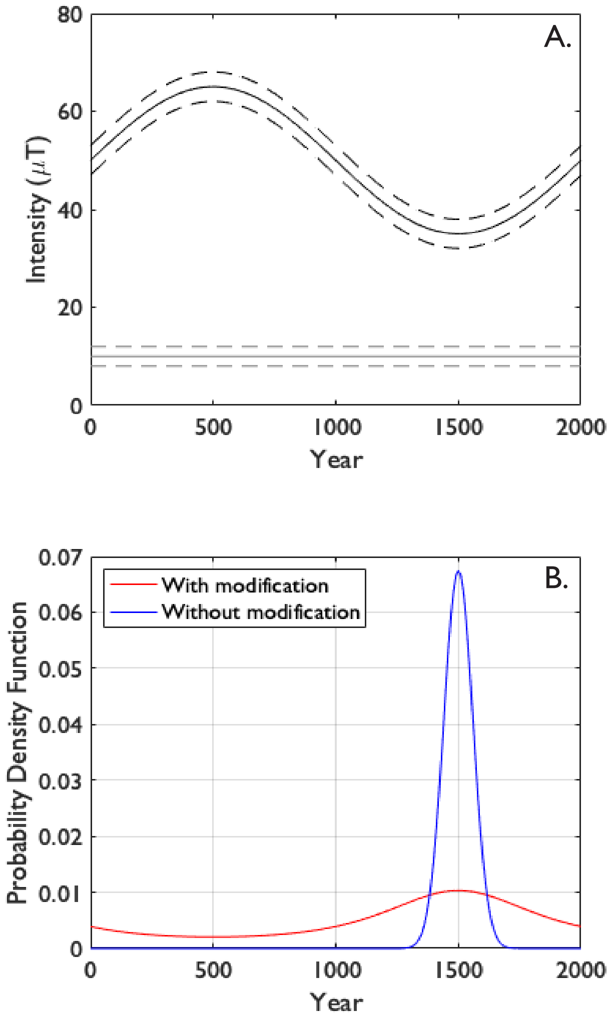

Figure 15: An example of accounting for unknown uncertainties with synthetic data. A. The grey line shows an archaeointensity estimate of 10 T and its associated error is shown in dashed lines. The black lines show a synthetic geomagnetic field model prediction (a sinusoidal curve) with its associated error is shown in dashed lines. B. The liklihood of ages for the archaeointensity estimate. The blue line shows the result that would be obtained using Lanos (2004) and Pavón-Carrasco et al. (2011). The red line shows how using an unknown uncertainty would affect the age estimate of a sample.

This modification is shown graphically in Figure 15 with synthetic data. The estimate and model do not intersect, which suggests that the data and/ or model likely have additional sources of error, which are not accounted for. By considering these unknown uncertainties in the dating method (Equation 3), a more suitable (non-informative) age estimate is given, which one should expect when model and data are so far apart from each other.

Figure 16A shows an example of this potential underestimation of uncertainties with the intensity results from the three different archaeointesity results from the Ness of Brodgar (Paper I) with the model pfm9k.2 (Nilsson et al., 2022) and ARCH-UK.1 (Batt et al., 2017). The analysed Ness of Brodgar site has well-defined ages, between 3000 BC - 2500 BC(see Figure 12) that are based on radiocarbon dates (Card et al., 2017) and can therefore be used to test the modified dating method and to evaluate the geomagnetic field models. Using the standard method of archaeomagnetic dating with pfm9k.2 (which is less consistent with the data than ARCH-UK.1) yields ages that are clearly inconsistent with the independent age estimates, whilst the modified method provides more conservative estimates. In the case of ARCH-UK.1, model and data are more consistent and both dating methods provide similar results.

Rate of Change of the Geomagnetic Field

Whilst we are unsure about how the geomagnetic field behaved in certain regions over archaeological time, we can likely obtain reasonably accurate information on the rate of change of the geomagnetic field based on comparisons to the present-day field (Davies & Constable, 2017). From satellite observations, we have a good understanding of what reasonable variations in the direction and strength of the field are expected over a certain period (Nilsson & Suttie, 2021). This is useful for cores, or other settings where there is stratigraphic information. This information can, for example be used to determine the minimum amount of time between each unit, that is likely to have passed to account for the geomagnetic field changes we observe from the archaeomagnetic investigation. The result gives an appropriate length of time for the creation of the entire core (or other material). If there are radiocarbon dates (or similar), it is possible to tie the results from the model to definite calendar years.

6.4. Outlook

With regards to the sites studied in this thesis, there are more Rangitoto samples (from below 80 m depth in the core) currently being analysed at the Palaeomagnetic

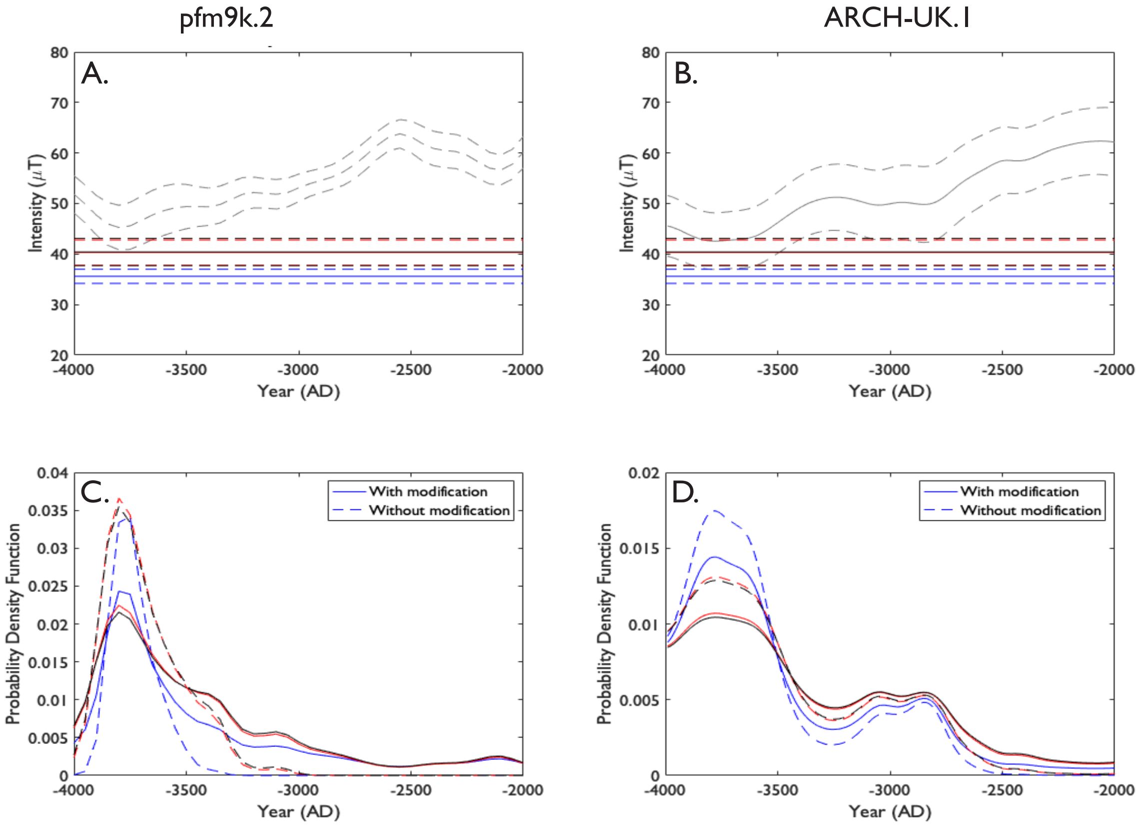

Figure 16: An archaeomagnetic dating example for the Ness of Brodgar with two different geomagnetic field models. A. shows the geomagnetic field prediction as per pfm9k.2 (Nilsson et al., 2022) with grey lines (the dashed lines show the 1σ envelope). The three archaeointensity estimates and associated error from the Ness of Brodgar in red, blue and black. B. Shows same information as A. but the geomagnetic field prediction is from ARCHUK.1 (Batt et al., 2017). C. The liklihood of ages for the archaeointensity estimates, using the same red, blue and black colours, from Ness of Brodgar (as per pfm9k.2). The dashed lines shows the result that would be obtained using Lanos (2004) and Pavón-Carrasco et al. (2011).The solid lines shows how an unknown uncertainty, such as in Kosareva et al. (2020) would affect the age estimate of a sample. D. Shows same information as C. but the age liklihood this time is gained from the ARCHUK.1 field model.

Laboratory at Lund University. Whilst we were able to draw conclusions from the data that was collected during this thesis work, this extra data would help to determine if the statistical modelling approach and age probabilities stated, remain correct. It must be noted that below approximately 115 m the mineralogy becomes more difficult for palaeointensity analysis so the focus of further measurements should be inclination measurements, in order to maximise the amount of new data that can be generated. If more palaeointensity experiments are ever conducted, they should focus on upper parts of the core to avoid the unfavourable mineralogy.

To provide more insight into geomagnetic field features, such as the SAA, it requires adding more data in the southern hemisphere. In addition to the work in this thesis there are many recent investigations (see Brown et al., 2021) providing new geomagnetic field information from the southern hemisphere (e.g.- Jaqueto et al., 2022; Trindade et al., 2018), although this is a time-consuming process. To maximise the data obtained from areas like these, one suggestion is to use sample level data to constrain the geomagnetic field models. This would result in less rejection of data (e.g.- if a site did not produce enough intensity estimates to make a reliable average) and potentially also enable a more appropriate propagation of data uncertainties into the models (see Figure 6, in appendixed Paper II, e.g.- by using a modified error distribution from Equation 3).

7. Conclusions

The first aim of this thesis was to add data to the archaeomagnetic record, especially where there is a scarcity, either chronologically or geographically (or both). New data has been collected, including the first archaeointensity data for the entire British Neolithic period in the UK.

Especially when considering older samples, the success rate can be low when completing archaeomagnetic experiments, but it is still possible to determine archaeomagnetic information. Using non-ideal samples is more laborious but opens up a wealth of new material for potential analysis.

The second aim was to refining the chronology of some of the studied sites if possible. Often data sparse areas are difficult to date using archaeomagnetic methods, but I have shown it is still possible to gain chronological information, by introducing alternative methodologies. Finally multiple reference curves should be considered when using archaeomagnetic dating.

Table 3: Author contributions to the papers that are compiled in this thesis. Non-author contributions are marked in italics. * indicates BSc projects co-supervised by A. Nilsson and M. L. Allington.

Task	Paper I (Ness of Brodgar)	Paper II (Southern Africa)	Paper III (Rangitoto Island Volcano)
Study Design	M. L. Allington C. M. Batt M. J. Hill	M. L. Allington A. Nilsson	P. C. Augustinus A. Nilsson M. L. Allington
Providing Material for Analysis	N. Card *R. Towers*	A. Lindahl *A. Antonites* *S. M. Mothulatshipi* *S. Khomalo*	P. C. Augustinus
Sampling	M. L. Allington *E. Hurst*	M. L. Allington A. Lindahl	M. L. Allington N. Suttie
Laboratory Analysis	M. L. Allington	M. L. Allington	M. L. Allington N. Suttie D. Daniil I. Hjorth* L. Aulin*
Data Interpretation	M. L. Allington C. M. Batt M. J. Hill A. Nilsson	M. L. Allington A. Nilsson	M. L. Allington A. Nilsson M. J. Hill D. Daniil
Statistical Modelling	-	M. L. Allington A. Nilsson	A. Nilsson
Writing of Original Manuscript Draft	M.L. Allington	M.L. Allington	M. L. Allington A. Nilsson
Preparation of Figures	M. L. Allington A. Nilsson	A. Nilsson M. L. Allington	A. Nilsson M.L. Allington
Review of Manuscript	All authors	All authors	All authors

Svensk Sammanfattning

Variationer i jordens magnetfält har uppmätts över hundratals år, från magnetiska observatorier till havs för navigeringsändamål noterade i skeppsloggar till dagens realtidsobservationer från satelliter. Sådana historiska mätdata har gjort det möjligt att rekonstruera förändringar i jordens magnetfält de senaste 400 åren. För att studera variationer i magnetfältet över längre tidskalor (från hundratals till tusentals år) är det nödvändigt att använda indirekta observationer av jordens magnetfält från till exempel vulkaniska bergarter eller upphettade/brända arkeologiska fynd. Rekonstruktioner av det jordmagnetiska fältet baserade på sådana arkeo-/paleomagnetiska data kan användas både för att datera arkeologiska och geologiska material samt för att studera processer i jordens kärna där fältet genereras.

För närvarande är de tillgängliga arkeo-/paleomagnetiska data varken geografiskt eller kronologiskt välfördelade. Det första målet med den här avhandlingen är därför att producera nya mätdata från platser som är underrepresenterade (antingen spatialt eller temporärt) i nuvarande arkeomagnetiska datakompilationer, vilket inkluderar södra Afrika, Nya Zeeland och Orkneyöarna, Storbritannien. Nya mätdata av variationer i jordensmagnetfälts intensitet från de tre utvalda områdena samt av variationer i magnetfältets riktning från Nya Zeeland har genererats. Att använda arkeomagnetiska rekonstruktioner i dateringssyfte kan vara utmanande i områden som dessa där referensdata till stor del saknas, eftersom det leder till stora och ofta okända osäkerheter i de arkeomagnetiska referenskurvorna. Det andra målet med den här avhandlingen är att åtgärda sådana problem genom att introducera alternativa metoder för arkeomagnetisk datering, som att (i) inkorporera de okända osäkerheterna i beräkningarna samt att (ii) använda alternativa mer tillförlitliga referensdata, såsom information om hur snabbt magnetfältet kan förändras, för att erhålla ny kronologisk information.

Popular Science Summary

The Earth's magnetic (geomagnetic) field is generated from deep inside the Earth's core, but we can still see the effects of it on the surface (e.g.- navigating using a compass) and even benefit from it as it provides a barrier to stop harmful energetic charged particles from space entering into Earth's atmosphere. However, in recent years the magnetic field has been getting weaker, especially around the South Atlantic region, known as the South Atlantic Anomaly. This has started to cause some issues as energetic particles in this region are now able to reach and interfere with objects in low-orbit around the Earth, e.g.- causing damage to satellites.

In order to fully understand the South Atlantic Anomaly, more measurements of the geomagnetic field are needed to reconstruct how it has evolved through time. Before satellite measurements and historical records (which are available for the past four centuries), it is still possible to get geomagnetic field measurements from signals recorded by the magnetic minerals in archaeological artefacts and volcanic rocks. However, our current databases lack records in the Southern Hemisphere, and also lack older measurements from time periods before 0 AD. This project has collected additional geomagnetic field data over archaeological times from the Southern Hemisphere, from both southern Africa and New Zealand. Additionally, the first geomagnetic field strength measurements for the Neolithic period in the United Kingdom (which occurred between 6000 to 4000 years ago) have been determined.

In addition to providing information about geomagnetic field evolution, geomagnetic field models constructed using sufficient measurement data can also be used to date archaeological artefacts and volcanic rocks of unknown age. The magnetic field recording extracted experimentally from the object under investigation can be matched to an appropriate model in order to tell us the age of said object. This project has shown it is possible to refine an object's age, even in areas where there are very few geomagnetic field measurements, thus providing valuable information, especially to archaeological excavations in the Southern Hemisphere.

References

Aidona, E., Kondopoulou, D., Kyriakidou, E. G., Camps, P., Sarafidis, C., Polymeris, G. S., & Orgeolet, R. (2023). Geomagnetic field intensity variations during the second millennium BCE: new data from the greek middle and late bronze age. Physics of the Earth and Planetary Interiors, 334, 106958. https://doi.org/10.1016/j.pepi.2022.106958

Aitken, M. J., Allsop, A. L., Bussell, G. D., & Winter, M. B. (1988). Determination of the intensity of the Earth's magnetic field during archaeological times: Reliability of the Thellier Technique. Reviews of Geophysics, 26(1), 3-12. https://doi.org/10.1029/RG026i001p00003

Aubert, J., Finlay, C. C., & Fournier, A. (2013). Bottom-up control of geomagnetic secular variation by the Earth's inner core. Nature, 502(7470), 219-223. https://doi.org/10.1038/nature12574

Baker, E. B., & Muxworthy, A. R. (2023). Using Preisach Theory to Evaluate Chemical Remanent Magnetization and Its Behavior During Thellier-Thellier-Coe Paleointensity Experiments. Journal of Geophysical Research: Solid Earth, 128(2), e2022JB025858. https://doi.org/10.1029/2022JB025858

Barbetti, M. F., McElhinny, M. W., Edwards, D. J., & Schmidt, P. W. (1977). Weathering processes in baked sediments and their effects on archaeomagnetic field-intensity measurements. Physics of the Earth and Planetary Interiors, 13(4), 346-354. https://doi.org/10.1016/0031-9201(77)90121-2

Batt, C. M., Brown, M. C., Clelland, S.-J., Korte, M., Linford, P., & Outram, Z. (2017). Advances in archaeomagnetic dating in Britain: New data, new approaches and a new calibration curve. Journal of Archaeological Science, 85, 66-82. https://doi.org/10.1016/j.jas.2017.07.002

Ben-Yosef, E., Tauxe, L., Ron, H., Agnon, A., Avner, U., Najjar, M., & Levy, T. E. (2008). A new approach for geomagnetic archaeointensity research: insights on ancient metallurgy in the Southern Levant. Journal of Archaeological Science, 35(11), 2863-2879. https://doi.org/10.1016/j.jas.2008.05.016

Biggin, A. J., Perrin, M., & Dekkers, M. J. (2007). A reliable absolute palaeointensity determination obtained from a non-ideal recorder. Earth and Planetary Science Letters, 257(3), 545-563. https://doi.org/https://doi.org/10.1016/j.epsl.2007.03.017

Brown, M. C., Donadini, F., Korte, M., Nilsson, A., Korhonen, K., Lodge, A., Lengyel, S. N., & Constable, C. G. (2015). GEOMAGIA50.v3: 1. general structure and modifications to the archeological and volcanic database. Earth, Planets and Space, 67(1), 83. https://doi.org/10.1186/s40623-015-0232-0

Brown, M. C., Hervé, G., Korte, M., & Genevey, A. (2021). Global archaeomagnetic data: The state of the art and future challenges. Physics of the Earth and Planetary Interiors, 318, 106766. https://doi.org/10.1016/j.pepi.2021.106766

Butler, R. F. (1992). Magnetic domains to geologic terranes. Blackwell.

Cai, S., Tauxe, L., Wang, W., Deng, C., Pan, Y., Yang, L., & Qin, H. (2020). High-Fidelity Archeointensity Results for the Late Neolithic Period From Central China. Geophysical Research Letters, 47(10), e2020GL087625. https://doi.org/10.1029/2020GL087625

Card, N. (2012). The Ness of Brodgar. British Archaeology 128, 14-21.

Card, N. (2018). The Ness of Brodgar Uncovering Orkney's Neolithic Heart Current Archaeology 335, 20-28.

Card, N., Mainland, I., Timpany, S., Towers, R., Batt, C., Ramsey, C. B., Dunbar, E., Reimer, P., Bayliss, A., Marshall, P., & Whittle, A. (2017). To Cut a Long Story Short: Formal Chronological Modelling for the Late Neolithic Site of Ness of Brodgar, Orkney. European Journal of Archaeology, 21(2), 217-263. https://doi.org/10.1017/eaa.2016.29

Carrancho, Á., & Villalaín, J. J. (2011). Different mechanisms of magnetisation recorded in experimental fires: Archaeomagnetic implications. Earth and Planetary Science Letters, 312(1), 176-187. https://doi.org/https://doi.org/10.1016/j.epsl.2011.10.006

Casas, L., & Incoronato, A. (2007). Distribution analysis of errors due to relocation of geomagnetic data using the 'Conversion via Pole' (CVP) method: Implications on archaeomagnetic data. Geophysical Journal International, 169(2), 448-454. https://doi.org/10.1111/j.1365-246X.2007.03346.x

Casas, L., Shaw, J., Gich, M., & Share, J. A. (2005). High-quality microwave archaeointensity determinations from an early 18th century ad English brick kiln. Geophysical Journal International, 161(3), 653-661. https://doi.org/10.1111/j.1365-246X.2005.02631.x

Coe, R. S. (1967). The Determination of Paleo-Intensities of the Earth's Magnetic Field with Emphasis on Mechanisms which Could Cause Non-ideal Behavior in Thellier's Method. Journal of geomagnetism and geoelectricity, 19(3), 157-179. https://doi.

org/10.5636/jgg.19.157

Constable, C., Korte, M., & Panovska, S. (2016). Persistent high paleosecular variation activity in southern hemisphere for at least 10 000 years. Earth and Planetary Science Letters, 453, 78-86. https://doi.org/http://dx.doi.org/10.1016/j.epsl.2016.08.015

Cowie, T., & MacSween, A. (1999). Grooved Ware from Scotland: a review. In R. M. Cleal, A. (Ed.), Grooved Ware in Britain and Ireland (Vol. Neolithic Studies Group Seminar Papers 3). Oxbow Books.

Cromwell, G., Tauxe, L., Staudigel, H., & Ron, H. (2015). Paleointensity estimates from historic and modern Hawaiian lava flows using glassy basalt as a primary source material. Physics of the Earth and Planetary Interiors, 241, 44-56. https://doi.org/10.1016/j.pepi.2014.12.007

Crow, P. (2008). Mineral weathering in forest soils and its relevance to the preservation of the buried archaeological resource. Journal of Archaeological Science, 35(8), 2262-2273. https://doi.org/10.1016/j.jas.2008.02.008

Dang, T., Li, X., Luo, B., Li, R., Zhang, B., Pham, K., Ren, D., Chen, X., Lei, J., & Wang, Y. (2022). Unveiling the Space Weather During the Starlink Satellites Destruction Event on 4 February 2022. Space Weather, 20(8), e2022SW003152. https://doi.org/10.1029/2022SW003152

Davies, C., & Constable, C. (2017). Geomagnetic spikes on the core-mantle boundary. Nature Communications, 8(1), 15593. https://doi.org/10.1038/ncomms15593

Day, R., Fuller, M., & Schmidt, V. A. (1977). Hysteresis properties of titanomagnetites: Grain-size and compositional dependence. Physics of the Earth and Planetary Interiors, 13(4), 260-267. https://doi.org/10.1016/0031-9201(77)90108-X

de Groot, L. V., Biggin, A. J., Dekkers, M. J., Langereis, C. G., & Herrero-Bervera, E. (2013). Rapid regional perturbations to the recent global geomagnetic decay revealed by a new Hawaiian record. Nature Communications, 4(1), 2727. https://doi.org/10.1038/ncomms3727

de Groot, L. V., Pimentel, A., & Di Chiara, A. (2016). The multimethod palaeointensity approach applied to volcanics from Terceira: full-vector geomagnetic data for the past 50 kyr. Geophysical Journal International, 206(1), 590-604. https://doi.org/10.1093/gji/ggw095

Dearing, J. (1999). Magnetic susceptibility. Environmental magnetism: A practical guide, 35-62.

Dekkers, M. J., & Böhnel, H. N. (2006). Reliable absolute palaeointensities independent of magnetic domain state. Earth and Planetary Science Letters, 248(1), 508-517. https://doi.org/10.1016/j.epsl.2006.05.040

Di Chiara, A. (2020). Palaeosecular variations of the geomagnetic field in Africa during the Holocene: a review. Geological Society, London, Special Publications, 497(1), 127-141. https://doi.org/10.1144/SP497-2019-51

Di Chiara, A., & Pavón-Carrasco, F. J. (2022). A first regional model of the past Earth's magnetic field from Africa for the last 4000 years. Physics of the Earth and Planetary Interiors, 325, 106855. https://doi.org/10.1016/j.pepi.2022.106855

Downey, W. S., & Tarling, D. H. (1984). Archaeomagnetic dating of Santorini volcanic eruptions and fired destruction levels of late Minoan civilization. Nature, 309(5968), 519-523. https://doi.org/10.1038/309519a0

Dunlop, D. J., & Özdemir, O. (1997). Rock magnetism: fundamentals and frontiers. Cambridge University Press.

Dunlop, D. J., & West, G. F. (1969). An experimental evaluation of single domain theories. Reviews of Geophysics, 7(4), 709-757. https://doi.org/10.1029/RG007i004p00709

Finlay, C. C., Aubert, J., & Gillet, N. (2016). Gyre-driven decay of the Earth's magnetic dipole. Nature Communications, 7(1), 10422. https://doi.org/10.1038/ncomms10422

Finlay, C. C., & Jackson, A. (2003). Equatorially Dominated Magnetic Field Change at the Surface of Earth's Core. Science, 300(5628), 2084-2086. https://doi.org/10.1126/science.1083324

Fox, J. M. W., & Aitken, M. J. (1980). Cooling-rate dependence of thermoremanent magnetisation. Nature, 283(5746), 462-463. https://doi.org/10.1038/283462a0

Francés-Negro, M., Carrancho, Á., Pérez-Romero, A., Arsuaga, J. L., Carretero, J. M., & Iriarte, E. (2019). Storage or cooking pots? Inferring pottery use through archaeomagnetic assessment of palaeotemperatures. Journal of Archaeological Science, 110, 104992. https://doi.org/10.1016/j.jas.2019.104992

Friis-Christensen, E., Lühr, H., & Hulot, G. (2006). Swarm: A constellation to study the Earth's magnetic field. Earth, Planets and Space, 58(4), 351-358. https://doi.org/10.1186/BF03351933

Glatzmaier, G. A., & Roberts, P. H. (1995). A three-dimensional convective dynamo solution with rotating and finitely conducting inner core and mantle. Physics of the Earth and Planetary Interiors, 91(1), 63-75. https://doi.org/10.1016/0031-9201(95)03049-3

Gómez-Paccard, M., & Pavón-Carrasco, F. J. (2018). Archaeomagnetism. In The Encyclopedia of Archaeological Sciences (pp. 1-5). https://doi.org/10.1002/9781119188230.saseas0036

González-López, A., Osete, M. L., Campuzano, S. A., Molina-Cardín, A., Rivera, P., & Pavón-Carrasco, F. J. (2021). Eccentric Dipole Evolution during the Last Reversal, Last Excursions, and Holocene Anomalies. Interpretation Using a 360-Dipole Ring Model. Geosciences, 11(11).

Grappone, J. M., Biggin, A. J., & Hill, M. J. (2019). Solving the mystery of the 1960 Hawaiian lava flow: implications for estimating Earth's magnetic field. Geophysical Journal International, 218(3), 1796-1806. https://doi.org/10.1093/gji/ggz252

Gubbins, D., Alfè, D., Davies, C., & Pozzo, M. (2015). On core convection and the geodynamo: Effects of high electrical and thermal conductivity. Physics of the Earth and Planetary Interiors, 247, 56-64. https://doi.org/10.1016/j.pepi.2015.04.002

Gubbins, D., Willis, A. P., & Sreenivasan, B. (2007). Correlation of Earth's magnetic field with lower mantle thermal and seismic structure. Physics of the Earth and Planetary Interiors, 162(3), 256-260. https://doi.org/10.1016/j.pepi.2007.04.014

Heirtzler, J. R. (2002). The future of the South Atlantic anomaly and implications for radiation damage in space. Journal of Atmospheric and Solar-Terrestrial Physics, 64(16), 1701-1708. https://doi.org/10.1016/S1364-6826(02)00120-7

Hellio, G., & Gillet, N. (2018). Time-correlation-based regression of the geomagnetic field from archeological and sediment records. Geophysical Journal International, 214(3), 1585-1607. https://doi.org/10.1093/gji/ggy214

Hervé, G., Chauvin, A., & Lanos, P. (2013a). Geomagnetic field variations in Western Europe from 1500BC to 200AD. Part I: Directional secular variation curve. Physics of the Earth and Planetary Interiors, 218, 1-13. https://doi.org/10.1016/j.pepi.2013.02.002

Hervé, G., Chauvin, A., & Lanos, P. (2013b). Geomagnetic field variations in Western Europe from 1500BC to 200AD. Part II: New intensity secular variation curve. Physics of the Earth and Planetary Interiors, 218, 51-65. https://doi.org/10.1016/j.pepi.2013.02.003

Hill, M. J., Gratton, M. N., & Shaw, J. (2002). A comparison of thermal and microwave palaeomagnetic techniques using lava containing laboratory induced remanence. Geophysical Journal International, 151(1), 157-163. https://doi.org/10.1046/j.1365-246X.2002.01745.x

Hill, M. J., & Shaw, J. (1999). Palaeointensity results for historic lavas from Mt Etna using microwave demagnetization/remagnetization in a modified Thellier-type experiment. Geophysical Journal International, 139(2), 583-590. https://doi.org/10.1046/j.1365-246x.1999.00980.x

Hill, M. J., & Shaw, J. (2000). Magnetic field intensity study of the 1960 Kilauea lava flow, Hawaii, using the microwave palaeointensity technique. Geophysical Journal International, 142(2), 487-504. https://doi.org/10.1046/j.1365-246x.2000.00164.x

Hoffman, K. A., & Biggin, A. J. (2005). A rapid multiple-sample approach to the determination of absolute paleointensity. Journal of Geophysical Research: Solid Earth, 110(B12). https://doi.org/10.1029/2005JB003646

Hoye, G. S. (1981). Archaeomagnetic secular variation record of Mount Vesuvius. Nature, 291(5812), 216-218. https://doi.org/10.1038/291216a0

Hrouda, F. (1994). A technique for the measurement of thermal changes of magnetic susceptibility of weakly magnetic rocks by the CS-2 apparatus and KLY-2 Kappabridge. Geophysical Journal International, 118(3), 604-612. https://doi.org/10.1111/j.1365-246X.1994.tb03987.x

Huder, L., Gillet, N., Finlay, C. C., Hammer, M. D., & Tchoungui, H. (2020). COV-OBS.x2: 180 years of geomagnetic field evolution from ground-based and satellite observations. Earth, Planets and Space, 72(1), 160. https://doi.org/10.1186/s40623-020-01194-2

Jackson, A., Jonkers, A. R., & Walker, M. R. (2000). Four centuries of geomagnetic secular variation from historical records. Philosophical Transactions of the Royal Society of London. Series A: Mathematical, Physical and Engineering Sciences, 358(1768), 957-990.

Jaqueto, P., Trindade, R. I. F., Terra-Nova, F., Feinberg, J. M., Novello, V. F., Stríkis, N. M., Schroedl, P., Azevedo, V., Strauss, B. E., Cruz, F. W., Cheng, H., & Edwards, R. L. (2022). Stalagmite paleomagnetic record of a quiet mid-to-late Holocene field activity in central South America. Nature Communications, 13(1), 1349. https://doi.org/10.1038/s41467-022-28972-8

Kapper, L., Serneels, V., Panovska, S., Ruíz, R. G., Hellio, G., Groot, L. d., Goguitchaichvili, A., Morales, J., & Ruíz, R. C. (2020). Novel insights on the geomagnetic field in West Africa from a new intensity reference curve (0-2000 AD). Scientific Reports, 10(1), 1121. https://doi.org/10.1038/s41598-020-57611-9

Karacic, S., Jameson, M., & Weil, A. B. (2016). A Burning Issue: Firing Temperatures and the Production of Late Bronze Age Pottery from Tarsus-Gözlükule, Turkey. Journal of Archaeological Science: Reports, 9, 599-607. https://doi.org/10.1016/j.jasrep.2016.08.046

Kermode, L. O. (1992). Geology of the Auckland urban area. Scale 1:50 000. IGNS, Lower Hutt.

Kirschvink, J. L. (1980). The least-squares line and plane and the analysis of palaeomagnetic data. Geophysical Journal International, 62(3), 699-718. https://doi.org/10.1111/j.1365-246X.1980.tb02601.x

Koenigsberger, J. G. (1938). Natural residual magnetism of eruptive rocks. Terrestrial Magnetism and Atmospheric Electricity, 43(3), 299-320. https://doi.org/10.1029/TE043i003p00299

Kondopoulou, D., Gómez-Paccard, M., Aidona, E., Rathossi, C., Carvallo, C., Tema, E., Efthimiadis, K. G., & Polymeris, G. S. (2017). Investigating the archaeointensity determination success of prehistoric ceramics through a multidisciplinary approach: new and re-evaluated data from Greek collections. Geophysical Journal International, 210(3), 1450-1471. https://doi.org/10.1093/gji/ggx224

Kono, M., & Ueno, N. (1977). Paleointensity determination by a modified thellier method. Physics of the Earth and Planetary Interiors, 13(4), 305-314. https://doi.org/10.1016/0031-9201(77)90114-5

Korte, M., Brown, M. C., Gunnarson, S. R., Nilsson, A., Panovska, S., Wardinski, I., & Constable, C. G. (2019). Refining Holocene geochronologies using palaeomagnetic records. Quaternary Geochronology, 50, 47-74. https://doi.org/10.1016/j.quageo.2018.11.004

Kosareva, L. R., Kuzina, D. M., Nurgaliev, D. K., Sitdikov, A. G., Luneva, O. V., Khasanov, D. I., Suttie, N., & Spassov, S. (2020). Archaeomagnetic investigations in Bolgar (Tatarstan). Studia Geophysica et Geodaetica, 64(2), 255-292. https://doi.org/10.1007/s11200-019-0493-3

Kostadinova-Avramova, M., & Jordanova, N. (2019). Study of cooling rate effect on baked clay materials and its importance for archaeointensity determinations. Physics of the Earth and Planetary Interiors, 288, 9-25. https://doi.org/10.1016/j.pepi.2019.02.009

Kostadinova-Avramova, M., Kovacheva, M., Boyadzhiev, Y., & Hervé, G. (2020). Archaeomagnetic knowledge of the Neolithic in Bulgaria with emphasis on intensity changes. Geological Society, London, Special Publications, 497(1), 89-111. https://doi.org/10.1144/SP497-2019-48

Kovacheva, M., Chauvin, A., Jordanova, N., Lanos, P., & Karloukovski, V. (2009). Remanence anisotropy effect on the palaeointensity results obtained from various archaeological materials, excluding pottery. Earth, Planets and Space, 61(6), 711-732. https://doi.org/10.1186/BF03353179

Kovacheva, M., Kostadinova-Avramova, M., Jordanova, N., Lanos, P., & Boyadzhiev, Y. (2014). Extended and revised archaeomagnetic database and secular variation curves from Bulgaria for the last eight millennia. Physics of the Earth and Planetary Interiors, 236, 79-94. https://doi.org/10.1016/j.pepi.2014.07.002

Krása, D., & Herrero-Bervera, E. (2005). Alteration induced changes of magnetic fabric as exemplified by dykes of the Koolau volcanic range. Earth and Planetary Science Letters, 240(2), 445-453. https://doi.org/10.1016/j.epsl.2005.09.028

Lanos, P. (2004). Bayesian Inference of Calibration Curves: Application to Archaeomagnetism. In C. E. Buck & A. R. Millard (Eds.), Tools for Constructing Chronologies: Crossing Disciplinary Boundaries (pp. 43-82). Springer London. https://doi.org/10.1007/978-1-4471-0231-1_3

Lanza, R., & Meloni, A. (2006). The Earth's magnetism (Vol. 280). Springer.

Lindsay, J. M., Leonard, G. S., Smid, E. R., & Hayward, B. W. (2011). Age of the Auckland Volcanic Field: a review of existing data. New Zealand Journal of Geology and Geophysics, 54(4), 379-401. https://doi.org/10.1080/00288306.2011.595805

Linford, P. (2006). Archaeomagnetic Dating: guidelines on producing and interpreting archaeomagnetic dates. English Heritage.

Linnell, T., Shane, P., Smith, I., Augustinus, P., Cronin, S., Lindsay, J., & Maas, R. (2016). Long-lived shield volcanism within a monogenetic basaltic field: the conundrum of Rangitoto volcano, New Zealand. Bulletin, 128(7-8), 1160-1172.

Lohmann, K. J., Goforth, K. M., Mackiewicz, A. G., Lim, D. S., & Lohmann, C. M. F. (2022). Magnetic maps in animal navigation. Journal of Comparative Physiology A, 208(1), 41-67. https://doi.org/10.1007/s00359-021-01529-8

Lowrie, W., & Alvarez, W. (1981). One hundred million years of geomagnetic polarity history. Geology, 9(9), 392-397. https://doi.org/10.1130/0091-7613(1981)

Merrill, R. T., & McFadden, P. L. (1994). Geomagnetic field stability: Reversal events and excursions. Earth and Planetary Science Letters, 121(1), 57-69. https://doi.org/10.1016/0012-821X(94)90031-0

Mound, J. E., & Davies, C. J. (2023). Longitudinal structure of Earth's magnetic field controlled by lower mantle heat flow. Nature Geoscience. https://

doi.org/10.1038/s41561-023-01148-9

Muscheler, R., Adolphi, F., Herbst, K., & Nilsson, A. (2016). The Revised Sunspot Record in Comparison to Cosmogenic Radionuclide-Based Solar Activity Reconstructions. Solar Physics, 291(9), 3025-3043. https://doi.org/10.1007/s11207-016-0969-z

Nagata, T., Arai, Y., & Momose, K. (1963). Secular Variation of the Geomagnetic Total Force during the Last 5000 Years. Journal of Geophysical Research (1896-1977), 68(18), 5277-5281. https://doi.org/https://doi.org/10.1029/j.2156-2202.1963.tb00005.x

Nagata, T., & Kobayashi, K. (1963). Thermo-chemical Remanent Magnetization of Rocks. Nature, 197(4866), 476-477. https://doi.org/10.1038/197476a0

Needham, A. J., Lindsay, J. M., Smith, I. E. M., Augustinus, P., & Shane, P. A. (2011). Sequential eruption of alkaline and sub-alkaline magmas from a small monogenetic volcano in the Auckland Volcanic Field, New Zealand. Journal of Volcanology and Geothermal Research, 201(1), 126-142. https://doi.org/https://doi.org/10.1016/j.jvolgeores.2010.07.017

Neukirch, L. P., Tarduno, J. A., Huffman, T. N., Watkeys, M. K., Scribner, C. A., & Cottrell, R. D. (2012). An archeomagnetic analysis of burnt grain bin floors from ca. 1200 to 1250 AD Iron-Age South Africa. Physics of the Earth and Planetary Interiors, 190-191, 71-79. https://doi.org/https://doi.org/10.1016/j.pepi.2011.11.004

Nguyen, L., Suttie, N., Nilsson, A., & Muscheler, R. (2022). A novel Bayesian approach for disentangling solar and geomagnetic field influences on the radionuclide production rates. Earth, Planets and Space, 74(1), 130. https://doi.org/10.1186/s40623-022-01688-1

Nilsson, A., Holme, R., Korte, M., Suttie, N., & Hill, M. (2014). Reconstructing Holocene geomagnetic field variation: new methods, models and implications. Geophysical Journal International, 198(1), 229-248. https://doi.org/10.1093/gji/ggu120

Nilsson, A., & Suttie, N. (2021). Probabilistic approach to geomagnetic field modelling of data with age uncertainties and post-depositional magnetisations. Physics of the Earth and Planetary Interiors, 317, 106737. https://doi.org/https://doi.org/10.1016/j.pepi.2021.106737

Nilsson, A., Suttie, N., Korte, M., Holme, R., & Hill, M. (2020). Persistent westward drift of the geomagnetic field at the core–mantle boundary linked to recurrent high-latitude weak/reverse flux patches. Geophysical Journal International, 222(2), 1423-1432. https://doi.org/10.1093/gji/ggaa249

Nilsson, A., Suttie, N., Stoner, J. S., & Muscheler, R. (2022). Recurrent ancient geomagnetic field anomalies shed light on future evolution of the South Atlantic Anomaly. Proceedings of the National Academy of Sciences, 119(24), e2200749119. https://doi.org/10.1073/pnas.2200749119

Oda, H., Shibuya, H., & Hsu, V. (2000). Palaeomagnetic records of the Brunhes/Matuyama polarity transition from ODP Leg 124 (Celebes and Sulu seas). Geophysical Journal International, 142(2), 319-338. https://doi.org/10.1046/j.1365-246x.2000.00130.x

Olson, P., & Amit, H. (2006). Changes in earth's dipole. Naturwissenschaften, 93(11), 519-542. https://doi.org/10.1007/s00114-006-0138-6

Pasquale, V. (2019). Curie temperature. Encyclopedia of solid earth geophysics, 1-2.

Paterson, G. A., Heslop, D., & Pan, Y. (2016). The pseudo-Thellier palaeointensity method: new calibration and uncertainty estimates. Geophysical Journal International, 207(3), 1596-1608. https://doi.org/10.1093/gji/ggw349

Paterson, G. A., Tauxe, L., Biggin, A. J., Shaar, R., & Jonestrask, L. C. (2014). On improving the selection of Thellier-type paleointensity data. Geochemistry, Geophysics, Geosystems, 15(4), 1180-1192. https://doi.org/10.1002/2013GC005135

Pavón-Carrasco, F. J., Campuzano, S. A., Rivero-Montero, M., Molina-Cardín, A., Gómez-Paccard, M., & Osete, M. L. (2021). SCHA.DIF.4k: 4,000 Years of Paleomagnetic Reconstruction for Europe and Its Application for Dating. Journal of Geophysical Research: Solid Earth, 126(3), e2020JB021237. https://doi.org/10.1029/2020JB021237

Pavón-Carrasco, F. J., Osete, M. L., Torta, J. M., & Gaya-Piqué, L. R. (2009). A regional archeomagnetic model for Europe for the last 3000 years, SCHA.DIF.3K: Applications to archeomagnetic dating. Geochemistry, Geophysics, Geosystems, 10(3). https://doi.org/10.1029/2008GC002244

Pavón-Carrasco, F. J., Rodríguez-González, J., Osete, M. L., & Torta, J. M. (2011). A Matlab tool for archaeomagnetic dating. Journal of Archaeological Science, 38(2), 408-419. https://doi.org/10.1016/j.jas.2010.09.021

Primdahl, F., Risbo, T., Merayo, J. M. G., Brauer, P., & Tøffner-Clausen, L. (2006). In-flight spacecraft magnetic field monitoring using scalar/vector gradiometry. Measurement Science and Technology, 17(6), 1563. https://doi.org/10.1088/0957-0233/17/6/038

Riisager, P., & Riisager, J. (2001). Detecting multidomain magnetic grains in Thellier palaeointensity experiments. Physics of the Earth and Planetary Interiors, 125(1), 111-117. https://doi.org/10.1016/S0031-9201(01)00236-9

Roberts, A. P., & Winklhofer, M. (2004). Why are geomagnetic excursions not always recorded in sediments? Constraints from post-depositional remanent magnetization lock-in modelling. Earth and Planetary Science Letters, 227(3), 345-359. https://doi.org/10.1016/j.epsl.2004.07.040

Rogers, J., Fox, J. M. W., & Aitken, M. J. (1979). Magnetic anisotropy in ancient pottery. Nature, 277(5698), 644-646. https://doi.org/10.1038/277644a0

Schanner, M., Korte, M., & Holschneider, M. (2022). ArchKalmag14k: A Kalman-Filter Based Global Geomagnetic Model for the Holocene. Journal of Geophysical Research: Solid Earth, 127(2), e2021JB023166. https://doi.org/10.1029/2021JB023166

Schnepp, E., Thallner, D., Arneitz, P., & Leonhardt, R. (2020b). New archeomagnetic secular variation data from Central Europe, II: Intensities. Physics of the Earth and Planetary Interiors, 309, 106605. https://doi.org/10.1016/j.pepi.2020.106605

Schnepp, E., Thallner, D., Arneitz, P., Mauritsch, H., Scholger, R., Rolf, C., & Leonhardt, R. (2020a). New archaeomagnetic secular variation data from Central Europe. I: directions. Geophysical Journal International, 220(2), 1023-1044. https://doi.org/10.1093/gji/ggz492

Shane, P., Gehrels, M., Zawalna-Geer, A., Augustinus, P., Lindsay, J., & Chaillou, I. (2013). Longevity of a small shield volcano revealed by crypto-tephra studies (Rangitoto volcano, New Zealand): Change in eruptive behavior of a basaltic field. Journal of Volcanology and Geothermal Research, 257, 174-183. https://doi.org/10.1016/j.jvolgeores.2013.03.026

Shaw, J. (1974). A New Method of Determining the Magnitude of the Palaeomagnetic Field: Application to five historic lavas and five archaeological samples. Geophysical Journal International, 39(1), 133-141. https://doi.org/10.1111/j.1365-246X.1974.tb05443.x

Sivia, D. (2006). Data analysis: a Bayesian tutorial. OUP Oxford.

Smith, P. J., & Needham, J. (1967). Magnetic declination in mediaeval China. Nature, 214, 1213-1214.

Tarduno, J. A., Watkeys, M. K., Huffman, T. N., Cottrell, R. D., Blackman, E. G., Wendt, A., Scribner, C. A., & Wagner, C. L. (2015). Antiquity of the South Atlantic Anomaly and evidence for top-down control on the geodynamo. Nature Communications, 6(1), 7865. https://doi.org/10.1038/ncomms8865

Tarling, D. H. (1983). Palaeomagnetism: Principles and Applications in Geology, Geophysics and Archaeology. Chapman and Hall.

Tauxe, L., Banerjee, S. K., F., B. R., & van der Voo, R. (2018). Essentials of Paleomagnetism

Tauxe, L., Mullender, T. A. T., & Pick, T. (1996). Potbellies, wasp-waists, and superparamagnetism in magnetic hysteresis. Journal of Geophysical Research: Solid Earth, 101(B1), 571-583. https://doi.org/10.1029/95JB03041

Tauxe, L., Pick, T., & Kok, Y. S. (1995). Relative paleointensity in sediments: A Pseudo-Thellier Approach. Geophysical Research Letters, 22(21), 2885-2888. https://doi.org/10.1029/95GL03166

Tauxe, L., & Staudigel, H. (2004). Strength of the geomagnetic field in the Cretaceous Normal Superchron: New data from submarine basaltic glass of the Troodos Ophiolite. Geochemistry, Geophysics, Geosystems, 5(2). https://doi.org/10.1029/2003GC000635

Tema, E., & Lanos, P. (2021). New Italian directional and intensity archaeomagnetic reference curves for the past 3000 years: Insights on secular variation and implications on dating. Archaeometry, 63(2), 428-445. https://doi.org/10.1111/arcm.12603

Thellier, E., & Thellier, O. (1959). Sur l'intensité du champ magnétique terrestre dans le passé historique et géologique. Annales de Geophysique, 15, 285. https://ui.adsabs.harvard.edu/abs/1959AnG....15..285T

Towers, R., & Card, N. (2015). Technological adaptation in Grooved Ware pottery from the Ness of Brodgar, Orkney, or how to make your cordons stick. Scottish Archaeological Journal, 36-37(1), 51-63. https://doi.org/10.3366/saj.2014.0050

Trindade, R. I. F., Jaqueto, P., Terra-Nova, F., Brandt, D., Hartmann, G. A., Feinberg, J. M., Strauss, B. E., Novello, V. F., Cruz, F. W., Karmann, I., Cheng, H., & Edwards, R. L. (2018). Speleothem record of geomagnetic South Atlantic Anomaly recurrence. Proceedings of the National Academy of Sciences, 115(52), 13198-13203. https://doi.org/10.1073/pnas.1809197115

Turner, G., de Gelder, G., Howarth, J., Greve, A., Kinger, R., Corkill, R., & Nilsson, A. (2015a). NZPSV1k and NZPSV10k: new palaeosecular variation master records from New Zealand: applications for dating and modelling. Abstracts/Proceedings of the Joint Assembly (AGU, GAC, MAC, CGU).

Turner, G. M., Howarth, J. D., de Gelder, G. I. N. O., & Fitzsimons, S. J. (2015b). A new high-resolution record of Holocene geomagnetic secular variation from New Zealand. Earth and Planetary Science Letters, 430, 296-307. https://doi.org/10.1016/j.epsl.2015.08.021

Turner, G. M., Kinger, R., McFadgen, B., & Gevers, M. (2020). The first archaeointensity records from New Zealand: evidence for a fifteenth century AD archaeomagnetic 'spike' in the SW Pacific Region? Geological Society, London, Special Publications, 497(1), 47-72. https://doi.org/10.1144/SP497-2019-71

van Velzen, A. J., & Zijderveld, J. D. A. (1995). Effects of weathering on single-domain magnetite in Early Pliocene marine marls. Geophysical Journal International, 121(1), 267-278. https://doi.org/10.1111/j.1365-246X.1995.tb03526.x

Verosub, K. L. (1977). Depositional and postdepositional processes in the magnetization of sediments. Reviews of Geophysics, 15(2), 129-143. https://doi.org/10.1029/RG015i002p00129

Yamamoto, Y. (2006). Possible TCRM acquisition of the Kilauea 1960 lava, Hawaii: failure of the Thellier paleointensity determination inferred from equilibrium temperature of the Fe–Ti oxide. Earth, Planets and Space, 58(8), 1033-1044. https://doi.org/10.1186/BF03352608

Yamamoto, Y., Tsunakawa, H., & Shibuya, H. (2003). Palaeointensity study of the Hawaiian 1960 lava: implications for possible causes of erroneously high intensities. Geophysical Journal International, 153(1), 263-276. https://doi.org/10.1046/j.1365-246X.2003.01909.x

Yu, Y., & Tauxe, L. (2005). Testing the IZZI protocol of geomagnetic field intensity determination. Geochemistry, Geophysics, Geosystems, 6(5). https://doi.org/10.1029/2004GC000840

Yu, Y., & Tauxe, L. (2006). Acquisition of viscous remanent magnetization. Physics of the Earth and Planetary Interiors, 159(1), 32-42. https://doi.org/10.1016/j.pepi.2006.05.002

Yu, Y., Tauxe, L., & Genevey, A. (2004). Toward an optimal geomagnetic field intensity determination technique. Geochemistry, Geophysics, Geosystems, 5(2). https://doi.org/10.1029/2003GC000630

Zananiri, I., Batt, C. M., Lanos, P., Tarling, D. H., & Linford, P. (2007). Archaeomagnetic secular variation in the UK during the past 4000 years and its application to archaeomagnetic dating. Physics of the Earth and Planetary Interiors, 160(2), 97-107. https://doi.org/10.1016/j.pepi.2006.08.006

Zhu, J., Zhang, Y., Wang, T., Zhao, C. H., Yu, J. C., Glascock, M. D., & Wang, C. S. (2014). Determining the Firing Temperature of Low-Fired Ancient Pottery: An Example from the Donghulin Site, Beijing, China. Archaeometry, 56(4), 562-572. https://doi.org/10.1111/arcm.12033

Printed by Media-Tryck, Lund 2023 NORDIC SWAN ECOLABEL 3041 0903

Quaternary Sciences
Department of Geology
Lund University
Sölvegatan 12
SE-223 62 Lund, Sweden
Telephone +46 46 222 78 80

ISSN 0281-3033
ISBN 978-91-87847-78-3